Modelling with Transport equations; chemotaxis and anisotropic diffusion

T. Hillen K.J. Painter A. Swan

August 30, 2014

Contents

1 Introduction to movement models

Many biological problems lend themselves well to mathematical models. Often we use these models to predict the behaviour of a population. We can attempt to predict only population size using ordinary differential equation models of the population dynamics, or attempt to predict spatial characteristics of the population through the use of partial differential equation models. In either case, certain simplifications are necessary. A key question which must be addressed when dealing with population models is how to obtain a model for the macroscopic behaviour of a population based on information about individuals in the population.

1.1 Measurements

As a first example, we consider the case of randomly moving individuals, and discuss how we may use information about these individuals to derive a model for the population. First, consider a random variable X_t which represents the location of an individual at time t. We can then consider two statistical measures as illustrated in Figure 1:

(A) **Population measurements:**

(A.1) Mean location: $\bar{X}_t = E(X_t)$, and

(A.2) Mean quadratic variation: $(\sum_{i=1}^{n}(X_{ti} - \bar{X}_t)^2)/(n-1) = V(X_t)$

These two measures represent characteristic values of the population based on averages of movement of their individuals. We can also consider characteristics of the individual particles themselves. We consider then:

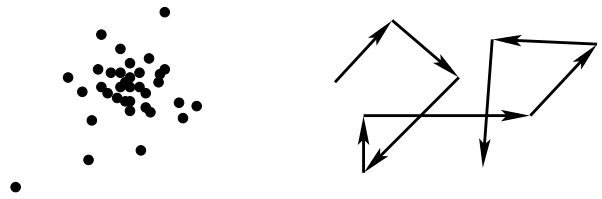

Figure 1: A: Schematic of individuals undergoing a random walk; the locations can be used to estimate a mean location and a mean squared displacement. B: Measurement of individual movement path for speed, turning rate and turning angle distribution
.

(B) **Individual measurements:**

(B.1) The mean speed, γ

(B.2) The mean turning rate, μ, and

(B.3) The distribution of newly chosen directions, $T(v, v')$, where v and v' are the new and previous velocities, respectively.

The final measure is often referred to as a kernel, and can be described as the probability of turning into velocity v given previous velocity v'. For a homogeneous environment, this will typically be a uniform distribution, but for directed environments, the distribution may not be uniform. For example, for a cancer cell moving within a brain, it will be more likely to turn into alignment with the fibrous brain structures then to travel orthogonally.

The aim of this manuscript is to develop mathematical models which are based on the above observations. In particular, we are interested in the following questions:

(Q1): How to make a mathematical model for these types of measurements?
(Q2): How are these models related?

1.2 Random walk on a grid

To derive a first and simple model on the population level, we first consider a random walker on a one dimensional grid [39, 29]. In this situation, consider an individual starting at point 0, and having some probability $0 < q < 1$ of moving to the right,

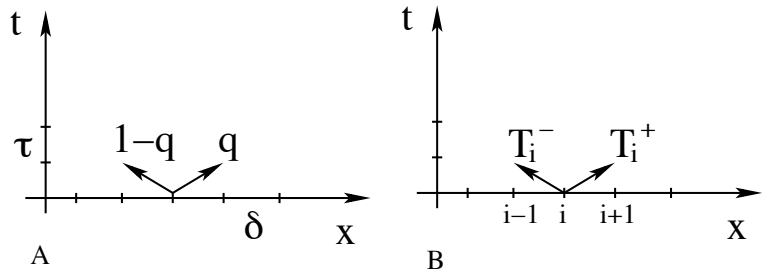

Figure 2: A: Simple random walk with constant jump probabilities q and $1-q$. B: Random walk with variable jump probabilities $T_i^{\pm}$.

and some probability $1-q$ of moving to the left. In this example, we assume that there is 0 probability of the random walker staying put. We let δ be the spatial step and τ be the time step. This situation is illustrated in Figure 2 (A).

We now consider X_n to be a random variable representing the position after n discrete steps. We can then compute the expected value of X_1 to be

$$E(X_1) = \sum_y xp(x=y) = \delta q + (-\delta)(1-q) = \delta(2q-1), \tag{1}$$

and thus we can recursively define $E(X_n)$ to be

$$E(X_n) = \delta(2q-1) + E(x_{n-1}) = n\delta(2q-1). \tag{2}$$

We now notice that if $q = \frac{1}{2}$ in equation 2, we have that $E(X_n) = 0$. This makes sense, as we would expect to find no net displacement when the probabilities for moving left and right are equal. If however $q > \frac{1}{2}$, then we have a higher probability of moving to the right, thus we would expect the net movement to be to the right. We see that in this case $E(X_n) > 0$, as expected. Conversely, when $q < \frac{1}{2}$, we have $E(X_n) < 0$, and see net movement to the left.

We can also consider the variance of our random variable. This is computed using the following formula:

$$V(X_1) = E(X_1^2) - E(X_1)^2. \tag{3}$$

We have $E(X_1)$ as computed in 1, so we easily have that $E(X_1)^2 = \delta^2(2q-1)^2$. We next compute

$$E(X_1^2) = \sum_y x^2 p(x=y) = \delta^2 q + (-\delta)^2(1-q) = \delta^2.$$

Therefore,

$$V(X_1) = \delta^2 - \delta^2(2q-1)^2 = 4\delta^2 q(1-q),$$

and subsequently,

$$V(X_n) = 4n\delta^2 q(1-q).$$

These measurements are for the discrete time situation, where an individual performs n jumps, $n \in \mathbb{N}$. How do these compare to the continuous time situation? If we consider a time step to have length τ, then $t = n\tau$ and $n = \frac{t}{\tau}$. We then define a mean velocity c and a diffusion constant D as:

$$c = \frac{E(X_t)}{t} = \frac{\delta}{\tau}(2q-1), \qquad D = \frac{1}{2}\frac{V(X_t)}{t} = \frac{2\delta^2}{\tau}q(1-q).$$

1.3 A continuous random walk

To derive a mathematical description of the random walk from above, we introduce $p(x,t)$ as probability density for the location of the random walker. We begin with a description of the discrete case discussed above. If we want to define an equation for $p(x, t+\tau)$, we are looking for the probability that an individual will be found at x when the time$= t+\tau$. We note that the only way for an individual to arrive at position x at time $t+\tau$, is to come from the grid point to the left, or to the right from time t. We use the **Master equation** approach

$$p(x, t+\tau) = qp(x-\delta, t) + (1-q)p(x+\delta, t), \tag{4}$$

where $q, 1-q$ are the probabilities for a jump to the right/left, respectively. In order to determine the continuous limit of this discrete equation, we will first take the expansion in the second variable of the right side about $t = \tau$, and the Taylor expansion with respect to the first variable about $x = \delta$, and $x = -\delta$. We remove the arguments (x,t), as all functions in this formula are evaluated at (x,t):

$$\begin{aligned} p + \tau p_t + \frac{\tau^2}{2}p_{tt} + \ldots &= q\left(p - \delta p_x + \frac{\delta^2}{2}p_{xx} - \ldots\right) \\ &\quad +(1-q)\left(p + \delta p_x + \frac{\delta^2}{2}p_{xx} + \ldots\right). \end{aligned}$$

Simplifying, we obtain

$$p_t(x,t) = \frac{\delta}{\tau}(1-2q)p_x(x,t) + \frac{\delta^2}{2\tau}p_{xx}(x,t) + \ldots. \tag{5}$$

We see that the dominating terms in equation 5 are the standard advection-diffusion equation with

$$c = \frac{\delta}{\tau}(1-2q) \quad \text{and} \quad D = \frac{\delta^2}{2\tau}.$$

At this stage we can study different possible limit scenarios for $\delta, \tau \to 0$ and $q \to 1/2$. We can do this in a number of ways, and we present three choices below. Of course, there are many more choices of these scalings, but most of them will not lead to a useful limit equation. In other words, if δ, τ, q do not scale as indicated below, then this method is not appropriate.

(a) $\frac{\delta}{\tau} \to \alpha$=constant. Then $\frac{\delta^2}{\tau} = \delta\frac{\delta}{\tau} \to 0$, which causes the diffusive term to vanish, and we are left with a simple **transport equation**

$$p_t = -cp_x.$$

(b) $\frac{\delta^2}{\tau} \to 2D$ =constant, then we can consider two cases:

(b.1) if $q = \frac{1}{2}$, then $c = 0$, and we obtain a pure **diffusion equation**

$$p_t = Dp_{xx}.$$

(b.2) If $q \to \frac{1}{2}$ in such a way that $\frac{\delta}{\tau}(1-2q) \to -c$, and $\frac{\delta^2}{2\tau} = \frac{D}{4q(1-q)} \to D$, then the scaling results in the **advection-diffusion equation**

$$p_t = -cp_x + Dp_{xx}, \tag{6}$$

where c and D are given by the measurements

$$c \approx \frac{E(X_t)}{t} \ , \ D \approx \frac{1}{2}\frac{V(X_t)}{t}.$$

Summary:

- When δ and τ scale in the same way, then we obtain a transport equation. This case is called **drift dominated**.
- When $\delta^2 \sim \tau$, we have the **diffusion dominated** case.
- Only if $q - \frac{1}{2} \sim \tau$ we get both terms, an advection and a diffusion term (**mixed case**).

1.4 Outline of this manuscript

2 A brief introduction to chemotaxis

Usually, authors are encouraged to find an objective voice and to avoid any form of excitement in a written text. Allow me, in this little introduction to chemotaxis, to do the opposite:

The phenomenon of chemotaxis has fascinated scientists since its first systematic investigation by biologists in the early 1900s. Chemotaxis describes tha active orientation of individuals, such as cells or baceria, on gradients of a chemical signal, which is produced by the cells themselves. In many examples, such as *Dictyostelium discoideum* (*DD*) or *Eschirichia coli*, this process leads to macroscopic cell aggregations. It is a prototype of self organization, where the resulting pattern is more than the sum of its parts. This is why so many people were excited about chemotaxis. Self organization is at the very heart of human existence. Everyone who has children has observed with fascination the wonder of embryonal development. The initial process of two cells coming together in the right environment to start embryogenesis is clear to most people, however, the development of two cells into a small little child is one of the unsolved mysteries of our existence and it lets us shiver in respect for this creation.

Chemotaxis offers a small glimpse into this process of self organization. It is now clear that many processes in embryogenesis are indeed driven by chemotactic responses. But also conceptually, chemotaxis offers a transition from an individual scale of moving cells to a macroscopic scale of a piece of tissue or an organ. And here comes the punch line for us mathematicians: Chemotaxis can be studied with mathematical models! This is a big development that was initiated by Patlack and by Keller and Segel. All of a sudden, mathematicians are no longer banned to the second row to observe biological experiemts from a distance - now, they are able to play a leading role in this field. How do patterns arise mathematically? Is blow-up the right framework? How can models be changed, adapted or improved? How do they relate to alternative models? etc.

Of course, the union of all mathematical chemotaxis papers since Keller and Segel in 1972 is huge, and it is not our intention to mention all important contributions. In fact, we will focus only at a few, selected, properties of chemotaxis. In particular those which are relevant to the modelling with transport equations, which is the topic of this manuscript. For further details we recommend the two review articles by Horstmann [21] and by Hillen and Painter [18].

Let's come back to a bit of history. Over the first twenty years on mathematical

chemotaxis studies, in particular in the 1990s, it has been shown that petri-dish experiments of chemotaxis of *E. coli, S. typhimurium* and also the slime molds *DD* can indeed be described by chemotaxis models. As such they are a clear success story of mathematical modelling. Hence scientists felt compelled to move back towards the first and original question - development of human organs, tissue and embryos. Many chemotaxis scientists have now advanced to study tissues and development. Another aspect of these topics are abnormalities such as cancer. Also cancer involves moving cells and chemotaxis and tumors share many characteristics with developing organs. Hence mathematical modelling of cancer has benefitted from the chemotaxis modelling as well. In this report, I will touch on many of these aspects which are the focus of much current research.

The modelling of cell movement also followed the fast developments of more and more advanced observation tools in biology. Confocal microscopy makes it possible to follow the movement of individual cells. All of a sudden, a new type of data becomes available. We are no longer measuring mean squared displacements, now we measure individual speeds, directions and turning angles. This information shall be used for chemotaxis as well, and it is here where transport equations enter the picture. Transport equations are a natural tool to use information about individual cell movement, and they can easily be adapted to model chemotaxis for example, or cancer invasion as well. Hence the focus of this manuscript are transport models and their applications. There is, of course, a close connection of transport models to chemotaxis models, and we will discuss those relations as well. They are classically known as *parabolic limit, hyperbolic limit*, or *moment closure methods*.

While transport equations for biological populations are the main focus here, chemotaxis will serve as a recurring example, where relevant assumptions are tested, and important results are illustrated. In the next few sections we first consider Keller and Segels classical motivation of the chemotaxis model (Section 2.1. Then we consider a random walk expressed by a master equation, that leads to chemotaxis in Section **??**. Two classical analysis methods will also be discussed, which is the often ignored linearisation of chemotaxis models in Section 2.3, and a cool method of Nanjundiah to study steady states in Section 2.4).

2.1 Random walk for chemotaxis

To describe the classical derivation of a chemotaxis model, as for example used by Keller and Segel [24], we first consider Fick's law of diffusion. The standard diffusion equation

$$u_t = D\Delta u,$$

has, by Fick's law, the population flux

$$J_{\text{diff}} = -D\nabla u. \tag{7}$$

Chemotaxis models can be based on the idea that chemical signals trigger a chemotactic flux which is proportional to the population density. As the population grows, so will the flux in response to the chemical signal. We can therefore describe the chemotactic flux, or J_{ch} to be $\beta \cdot u$, where u is the population density, and β is the associated rate, which will depend on the signal concentration $v(x,t)$, and will be directed in the direction of $\nabla v(x,t)$. This is because the particles prefer high concentrations of v, hence the particle flux is in direction of the gradient of v.

$$\beta = \chi(v)\nabla v,$$

where $\chi(v)$ is the *chemotactic sensitivity*. This means that as the cells become more sensitive to the chemical signal present, β will increase and in turn, so will the flux. Combining this chemotactic flux term with the diffusive flux in (7), we obtain the formula for the total flux:

$$J = -D\nabla u + \chi(v)u\nabla v. \tag{8}$$

This in turn gives us the diffusion based chemotactic model, given by the following coupled PDE system:

$$\begin{aligned} u_t &= \nabla\left(D\nabla u - \chi(v)u\nabla v\right) \\ v_t &= D_v\Delta v + f(v,u), \end{aligned} \tag{9}$$

where D_v is the diffusion coefficient of the chemical signal and $f(v,u)$ describes the production or consumption of the signal. For example, we might have $f(v,u) = -\alpha v + \gamma u$. This model is called the Patlak-Keller-Segel, or PKS model [18].

2.2 Derivation via master equation approach

It turns out that we can obtain the same PKS model (9) through derivation from a random walk, as was done in the previous Section 1.3. For a chemotaxis model, however, we cannot assume that the jump probabilities (q and $1-q$ in the above derivation) are constant in space. This is because for cells moving in response to a chemical gradient, the jump probabilities will depend on the signal strength, which will be spatially dependent. For an individual cell at position i, it will move to the left with probability T_i^- and will move right with probability T_i^+. The step size h is considered to be constant in space. This situation is illustrated in Figure 2 (B).

As before, we can derive an overall equation for the movement of individual cells. This is based again on the idea that cells can only move into location i from locations $i-1$ and $i+1$ with their respective probabilities, and move out of position i into the adjacent locations, again with the appropriate probabilities. The difference now is that the probabilities will be spatially dependent. The master equation then becomes

$$\frac{\partial u(x_i,t)}{\partial t} = T^+_{i-1}u_{i-1} + T^-_{i+1}u_{i+1} - (T^+_i + T^-_i)u_i, \tag{10}$$

where $u_i = u(x_i,t)$ is the cell density at location i. We want to now describe the jump probabilities as a function of the signal strength (v). As such, we will define v_i to be the signal strength at location x_i. The jump probability will also depend on the cell's ability to sense the signal present, hence we next define $\tau(v)$ to be the chemical mechanism to measure signal concentrations. For example in Section 2.2.1 we choose τ to be the number of bound surface receptors, which will depend on the chemical concentration. We then define the jump probabilities using the function τ, as well as two parameters, $\alpha > 0$ and $\beta \geq 0$ as

$$T^\pm_i = \alpha + \beta(\tau(v_{i\pm1}) - \tau(v_i)).$$

If we consider T^+_i for example, we see that the jump probability increases as compared to no signal, when $\tau(v_{i+1})$ is bigger than $\tau(v_i)$. Plugging these transitional probabilities $T^\pm_i$ into equation (10), we obtain

$$\begin{aligned}\frac{\partial u_i}{\partial t} &= \alpha(u_{i-1} + u_{i+1} - 2u_i) \\ &\quad +\beta[(\tau(v_i) - \tau(v_{i-1}))u_{i-1} + (\tau(v_i) - \tau(v_{i+1}))u_{i+1} \\ &\quad -(\tau(v_{i+1}) - \tau(v_i) + \tau(v_{i-1}) - \tau(v_i))u_i],\end{aligned}$$

which simplifies to

$$\begin{aligned}\frac{\partial u_i}{\partial t} &= \alpha(u_{i-1} + u_{i+1} - 2u_i) \\ &\quad +\beta((u_{i+1} + u_i)(\tau(v_i) - \tau(v_{i+1})) - (u_i + u_{i-1})(\tau(v_{i-1}) - \tau(v_i))).\end{aligned} \tag{11}$$

Intuitively, we expect that the jump probabilities should depend on the step size h. For example, if h is reduced, we expect $T^\pm_i$ to increase, as the cells have a higher probability of jumping a short distance than a long one. As such, we can define a new probabilities $\tilde{T}^\pm_i$ where the implicit dependence on h is made explicit. We then have $\tilde{T}^\pm_i = \frac{1}{h^2}T^\pm_i$ where k is an appropriate scaling constant. If we include this in equation (11), we obtain

$$\frac{\partial u_i}{\partial t} = \alpha \left(\frac{u_{i-1} + u_{i+1} - 2u_i}{h^2} \right) - \beta \frac{F_{i+1} - F_i}{h}, \tag{12}$$

where we introduced

$$F_i = (u_i + u_{i-1}) \frac{\tau(v_i) - \tau(v_{i-1})}{h}.$$

We now notice that equation (12) contains several approximations to derivatives. If we then take the limit as $h \to 0$, we get the following:

$$\begin{aligned} \frac{\partial u}{\partial t} &= \alpha \frac{\partial^2 u}{\partial x^2} - \beta \frac{\partial}{\partial x} \left(2u \frac{\partial \tau(v)}{\partial x} \right) \\ &= \alpha \frac{\partial^2 u}{\partial x^2} - \frac{\partial}{\partial x} \left(2\beta u \frac{\partial \tau}{\partial v} \frac{\partial v}{\partial x} \right), \end{aligned} \tag{13}$$

which is equivalent to

$$\frac{\partial u}{\partial t} = D \frac{\partial^2 u}{\partial x^2} - \frac{\partial}{\partial x} \left(\chi(v) u \frac{\partial v}{\partial x} \right) \tag{14}$$

with $D = \alpha$ and $\chi(v) = 2\beta \frac{\partial \tau}{\partial v}$. We see that equation (14) is the same as the first equation of (9) in one dimension. This shows that we can derive the chemotaxis equation both from a flux argument, and also from considering the individual random cell movements. We will encounter a third derivation when we study transport equations later.

2.2.1 Example: receptor kinetics

We choose an important biological application as an example. In a typical situation, the chemotactic signal will bind to external cell surface receptors. We use a mass action approach to model both the receptors, and the signal to which they respond. Let R denote the concentration of receptors on the cell surface which have not been activated, V denotes the chemical signal, and R_a the concentration of receptors on the cell surface which have been activated by the chemical signal.

The system, illustrated in Figure **??** is described by the chemical reaction

$$R + V \rightleftharpoons_{k^-}^{k^+} R_a,$$

with the receptors being activated at a rate of k^+, and the activated receptors becoming deactivated at a rate of k^-. The system is illustrated in Figure **??**.

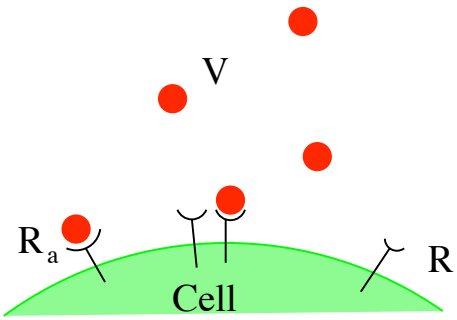

Figure 3: The system containing the cell surface receptors R, the activated receptors R_a and the chemical signal V. Receptors become activated at a rate of k^+ and deactivated at a rate of k^-.

Using mass action kinetics we obtain the following ODEs for the concentrations:

$$\begin{aligned}\frac{\partial R}{\partial t} &= k^- R_a - k^+ RV,\\ \frac{\partial V}{\partial t} &= k^- R_a - k^+ RV,\\ \frac{\partial R_a}{\partial t} &= k^+ RV - k^- R_a.\end{aligned}$$

The reaction is fast relative to cell movement, thus we consider the steady states of the system. For example, for R_a, we obtain

$$R_a = \frac{k^+}{k^-} RV,$$

in steady state. We also assume that the total number of receptors on the cell surface will remain constant, therefore $R + R_a = N$. Then $R = N - R_a$ and

$$R_a = \frac{k^+}{k^-}(N - R_a)V,$$

which gives

$$\left(1 + \frac{k^+}{k^-}V\right) R_a = \frac{k^+}{k^-} NV,$$

and so

$$R_a = \frac{\frac{k^+}{k^-}NV}{1 + \frac{k^+}{k^-}V}. \tag{15}$$

We can simplify equation (15) by defining $k := \frac{k^-}{k^+}$, giving

$$R_a = \frac{NV}{k+V}. \tag{16}$$

Recall from above that $\tau(v)$ is the chemical mechanism to measure signal concentrations. We said that $\tau(v)$ could be defined by the number of bound surface receptors, which will depend on the chemical concentration, hence $\tau(v) = R_a(v)$. Then we have

$$\tau'(v) = \frac{N(k+v) - Nv}{(k+v)^2} = \frac{Nk}{(k+v)^2},$$

and the chemotactic sensitivity in (9) becomes.

$$\chi(v) = \frac{C_1}{(k+v)^2}, \tag{17}$$

where C_1 is a constant.

2.3 Linearization of the classic chemotaxis model

The classical chemotaxis model has been analysed with more and more advanced methods, estimates and Lyapunov functions. A first step in this analysis is a linearisation around the homogeneous steady state. The linearisation leads already to a critical mass conditions, which plays an important role for blow-up results [21, 18].

We study the PKS model (9) for constant chemotacitc sensitivity χ and linear terms in the signal equation. This model has been denoted as the *minimal* chemotaxis model in [18].

$$\begin{aligned} u_t &= \nabla(\nabla u - \chi u \nabla v), \\ \varepsilon v_t &= D_v \Delta v + \alpha u - \beta v. \end{aligned} \tag{18}$$

We note that we have now incorporated a factor of ε with the time derivative of v. This coefficient comes from a rescaling of time. Since t corresponds to the time scale of cell movement, we adjust the time scale for the movement of the chemical signal by ε, implying that the chemical reactions are fast as compared to cell movement. We introduce $\tau = t/\varepsilon$ rescaling gives the system above. The model uses homogeneous Neumann, or zero flux boundary conditions $\nabla v = \nabla u = 0$ on the boundaries of a smooth bounded domain Ω. We will use a linearization in 1-D to study stability of a homogeneous steady state. This indicate either global existence of solutions or the

onset of spike formation. We first make a couple of observations about the model. Firstly, we see that it has spatially homogeneous equilibrium of (18 satisfies

$$\alpha\bar{u} = \beta\bar{v},$$

where α and β are constant, and $\bar{u}$ and $\bar{v}$ are the equilibrium distributions. We also note that the first equation obeys conservation of mass:

$$M := \int u(x,t)dt = C_2,$$

where C_2 is a constant. We thus have that the steady state distributions

$$\bar{u} = \frac{M}{|\Omega|} \quad \text{and } \bar{v} = \frac{\alpha}{\beta}\bar{u}.$$

To linearize (18) in $(\bar{u}, \bar{v})$ we rewrite the system as

$$\begin{aligned} u_t &= u_{xx} - \chi u_x v_x - \chi_u v + \chi u v_{xx},, \\ \varepsilon v_t &= D_v u_{xx} + \alpha u - \beta v. \end{aligned}$$

We let U and V be small perturbations and set $u = \bar{u} + U$, and $v = \bar{v} + V$. The derivatives are thus given by $u_x = U_x$, $u_{xx} = U_{xx}$, and $v_x = V_x$, $v_{xx} = V_{xx}$. Substituting these, the system becomes

$$U_t = U_{xx} - \chi\bar{u}V_{xx},, \tag{19}$$

$$\varepsilon V_t = D_v V_{xx} + \alpha U - \beta V. \tag{20}$$

Recall that $\bar{u} = \frac{M}{|\Omega|}$. Keeping this in mind and taking Fourier transforms with dual variable ω, we convert the differentiation to multiplication and write this as a linear system:

$$\begin{pmatrix} \hat{U} \\ \hat{V} \end{pmatrix}_t = \begin{pmatrix} -\omega^2 & \chi\frac{M}{|\Omega|}\omega^2 \\ \frac{\alpha}{\varepsilon} & -\omega^2\frac{D_v}{\varepsilon} - \frac{\beta}{\varepsilon} \end{pmatrix} \begin{pmatrix} U \\ V \end{pmatrix}.$$

We see that the trace of the coefficient matrix is

$$\text{tr} = -\omega^2\left(1 + \frac{D_v}{\varepsilon}\right) - \frac{\beta}{\varepsilon} < 0,$$

and the determinant is

$$\det = \omega^2 \left(\omega^2 \frac{D_v}{\varepsilon} + \frac{\beta}{\varepsilon} \right) - \frac{\alpha\chi M}{\varepsilon|\Omega|}\omega^2 = \frac{\omega^2}{\varepsilon} \left(\omega^2 D_v + \beta - \frac{\alpha\chi M}{|\Omega|} \right).$$

Since the trace is always < 0, we have either a saddle or a stable node. A saddle occurs when we have the existence of an unstable eigenvalue, i.e. when the determinant is negative. This condition is equivalent to

$$\omega^2 D_v < -\beta + \frac{\alpha\chi M}{|\Omega|}, \tag{21}$$

which gives the necessary condition for instability:

$$\frac{\alpha\chi M}{|\Omega|} > \beta. \tag{22}$$

Condition (22) gives a necessary condition for the existence of a saddle. Note that this condition is independent of ε. If we wish to find a sufficient condition, we must know the eigenvalues of the operator on the domain.

As an example, consider taking $\Omega = [0, \ell]$. The eigenvalues of the Laplacian on Ω with homogenous Neumann boundary conditions are

$$\omega_n = \frac{n\pi}{\ell}, \qquad n = 0, 1, 2, \ldots.$$

The condition given in (22) therefore becomes

$$\left(\frac{n\pi}{\ell}\right)^2 D_v < -\beta + \alpha\frac{\chi M}{|\Omega|}.$$

In order to have at least one nontrivial unstable mode ($n = 1$), we need

$$\frac{\pi^2}{\ell^2} D_v < -\beta + \alpha\frac{\chi M}{|\Omega|},$$

giving a sufficient condition for the formation of a saddle. If this condition is satisfied, then there exists a positive eigenvalue for the eigenfunction $\cos(\frac{\pi x}{\ell})$. The cosine grows with time and it might initiated the formation of a spike. A global analysis needs to be carried out to characterize the full spike formation.

2.4 Steady states

In this section we present a method from Nanjundiah [28] to study steady states for the chemotaxis model. The steady state equations are:

$$\begin{aligned} 0 &= \nabla(\nabla u - \chi u \nabla v), \\ 0 &= D_v \Delta v + \alpha u - \beta v. \end{aligned} \tag{23}$$

In [28], they use a clever trick for analyzing the steady states. First we define $\psi = ue^{-\chi v}$. Note that ψ is strictly positive and only 0 if $u = 0$. Then

$$\nabla\psi = \nabla u e^{-\chi v} - \chi \nabla v u e^{-\chi v} = (\nabla u - \chi \nabla v u)e^{-\chi v}.$$

Equation (**??**) then reads $\nabla(\nabla\psi e^{\chi v}) = 0$, which can be written as

$$\nabla\psi e^{\chi v} + \nabla\psi\chi\nabla v e^{\chi v} = 0,$$

and therefore we have

$$\Delta\psi + \chi\nabla\psi\nabla v = 0.$$

If for example our domain $\Omega \subseteq \mathbb{R}^2$ and has a smooth boundary, then the Hopf-maximum principle applies. This tells us that $\psi(x) = \text{const.} = \psi$ which means that $u(x) = \psi e^{\chi v(x)}$. As a consequence, u and v have the same maxima and minima. Moreover, it follows that

$$\nabla u - \chi u \nabla v = 0$$

on Ω. Now if we substitute $u(x)$ into equation (**??**), we obtain

$$0 = D_v \nabla v + \alpha\psi e^{\chi v} - \beta v, \tag{24}$$

which gives the governing equation for steady states.

In one spatial dimension, we can fully analyse the steady state equation (24):

$$D_v v'' + k e^{\chi v} - \beta v, \qquad k = \alpha\Psi.$$

Introducing $w := v'$ we can write the above equation as a first order system

$$\begin{aligned} v' &= w \\ w' &= -\tfrac{k}{D_v} e^{\chi v} + \tfrac{\beta}{D_v} v \end{aligned} \tag{25}$$

which is a 2-dimensional Hamiltonian system with Hamiltonian

$$H(v, w) = -\frac{w^2}{2} + \frac{\beta v^2}{2D_v} - \frac{k}{\chi d_v} e^{\chi v}.$$

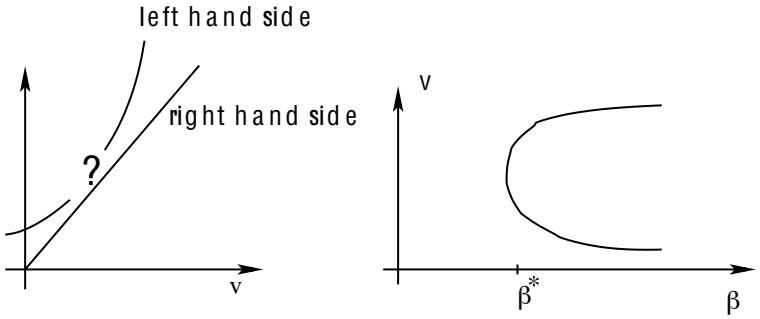

Figure 4: Left: sketch of the left hand side and the right hand side of (26) as functions of v. The question mark indicates the area where 0,1, or 2 intersections are possible. Right: sketch of the bifurcation diagram as function of β.

The equilibria of this Hamiltonian system satisfy $w = 0$ and

$$ke^{\chi v} = \beta v. \tag{26}$$

The left hand side and the right hand side are shown in Figure 4 (left) as functions of v. We see that depending on the values of the parameters, there are 0, 1, or 2 solutions to equation (26). A bifurcation occurs when the curves from the left hand side and from the right hand side of (26) touch. Hence the derivatives agree at a certain point v^* with:

$$k\chi e^{\chi v^*} = \beta \quad \text{and} \quad ke^{\chi v^*} = \beta v^*.$$

This implies that

$$\beta = \chi \beta v^*$$

and hence

$$v^* = \frac{1}{k}, \quad \text{and} \quad \beta^* = k\chi e,$$

where β^* is the critical value where this bifurcation occurs. If $\beta > \beta^*$ then we have two solutions $v_1 < \bar{v} < v_2$ of (26) (see Figure 4, right). If $\beta < \beta^*$, then we have no solution. This means that for $\beta > \beta^*$ we have two equilibria $(v_1, 0), (v_2, 0)$ of the Hamiltonian system (25). The Jacobian of (25) at a steady state $(v_i, 0)$ is

$$J(v_i, 0) = \begin{pmatrix} 0 & 1 \\ -\frac{k\chi}{D_v} e^{\chi v_i} + \frac{\beta}{D_v} & 0 \end{pmatrix},$$

with

$$\text{tr} = 0 \quad \text{and} \quad \det = \frac{k\chi}{D_v} e^{\chi v_i} - \frac{\beta}{D_v}.$$

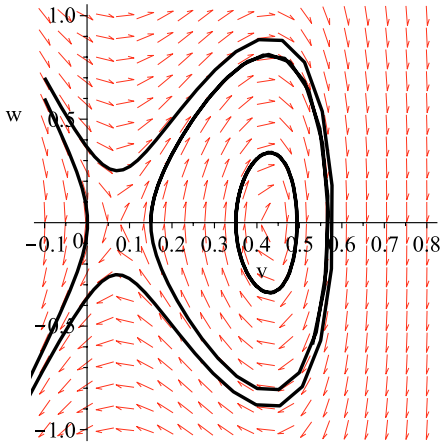

Figure 5: Phase portrait of the Hamiltonian system (25). The black lines indicate typical steady states of the chemotaxis model.

Hence the sign of the determinant is given by the sign of $k\chi e^{\chi v_i} - \beta$. At the smaller steady state v_1 the slope of $ke^{\chi v}$ is smaller than β, hence

$$k\chi e^{\chi v_1} < \beta$$

and $(v_1, 0)$ is a saddle point. For v_2 we find

$$k\chi e^{\chi v_2} > \beta$$

and $(v_2, 0)$ is a center. The phase portrait of the Hamiltonian system (25) is shown in Figure 5. Orbits rotate around the centre at $(v_2, 0)$ and the saddle at $(v_1, 0)$ connects to a homoclinic orbit. If system (24) would be considered with homogeneous Neumann boundary conditions on $[0, L]$, for example, then

$$w(0) = w(L) = 0$$

and steady states are solutions which start on the v-axis and end on the v-axis after exactly L units. As seen in Figure 5, these are solutions which have $1/2$ rotation, or one rotation or $3/2$ rotations etc. Solutions which pass close to the saddle at $(v_1, 0)$ are longer, while solutions near the centre $(v_2, 0)$ are shorter. We skip a full analysis of this system, which can be found in classical texts on dynamical systems.

3 Correlated random walk in one dimension

The one dimensional correlated random walk is an extension of the diffusion random walks studied earlier, as it allows for correlation of movement from one time step to the next; in particular correlation in velocity. These models are easy to understand and they form a basis for the understanding of higher dimensional transport equations. In fact, many of the abstract methods which we introduce later for transport equations, are simply illustrated in the one-dimensional context. However, the 1-D model is not only a motivating example, it is a valid model for random walk on its own and it has been applied to many interesting biological problems. See for example the review article of Eftimie [6] on animal swarming models.

In the following sections we will introduce the model and various equivalent variations, we will discuss suitable boundary conditions, and we will write the model in an abstract framework, which will become important later.

3.1 The Goldstein-Kac model in 1-D

Taylor [36] and Fuerth [8] developed the one dimensional correlated random walk model in the same year. Goldstein [11] and Kac [23] formulated it as a partial differential equation, and this is where we start. Let $u^{\pm}(x,t)$ denote the densities of right/left moving particles. The *Goldstein-Kac model* for correlated random walk is

$$\begin{aligned} u_t^+ + \gamma u_x^+ &= -\tfrac{\mu}{2}u^+ + \tfrac{\mu}{2}u^- \\ u_t^- - \gamma u_x^- &= \tfrac{\mu}{2}u^+ - \tfrac{\mu}{2}u^+, \end{aligned} \tag{27}$$

where γ denotes the (constant) particle speed and $\mu/2 > 0$ is the rate of switching directions from plus to minus or *vice versa*. We can also consider an equivalent formulation as a *one-dimensional transport equation*

$$\begin{aligned} u_t^+ + \gamma u_x^+ &= -\mu u^+ + \tfrac{\mu}{2}(u^+ + u^-) \\ u_t^- - \gamma u_x^- &= -\mu u^- + \tfrac{\mu}{2}(u^+ + u^-), \end{aligned} \tag{28}$$

where now $\mu > 0$ is the rate of directional changes; new directions are chosen as plus or minus with equal probability 1/2.

Another equivalent formulation arises if we look at the total population $u = u^+ + u^-$ and the population flux $v = \gamma(u^+ - u^-)$:

$$\begin{aligned} u_t + v_x &= 0 \\ v_t + \gamma^2 u_x &= -\mu v, \end{aligned} \tag{29}$$

which is also known as *Cattaneo system*. This formulation will be more natural for scientists with experience in continuum mechanics, as the first equation is a conservation of mass equation, while the second equation can be seen as a momentum equation, where the flux adapts to the negative population gradient with a time factor or $e^{-\mu t}$. See Joseph and Preziosi [22] for a detailed connection to continuum mechanics and to media with memory. Here, we stay with the interpretation of population models.

If we assume the solutions are twice continuously differentiable, we get yet another closely related equation. Indeed, differentiating the first equation of (29) by t and the second by x we get

$$\begin{aligned} u_{tt} + v_{xt}^{+} &= 0 \\ v_{xt} + \gamma^2 u_{xx} &= -\mu v_x, \end{aligned} \tag{30}$$

which can be rearranged into an equation for u alone:

$$\frac{1}{\mu} u_{tt} + u_t = \frac{\gamma^2}{\mu} u_{xx}, \tag{31}$$

which is the *telegraph equation*. This equation can be derived for the electrical potential along a transatlantic telegraph cable; a quite astonishing relation for our original random walk model. In this equation we then clearly see the relation to a diffusion equation. Just imagine that $\mu \to \infty$ and we loose the second time derivative term. At the same time we let $\gamma \to \infty$ such that

$$0 < \lim_{\gamma \to \infty, \mu \to \infty} \frac{\gamma^2}{\mu} =: D < \infty.$$

Then D becomes the diffusion coefficient and the parabolic limit equation reads

$$u_t = D u_{xx}.$$

We see that the one-dimensional model for correlated random walk is in fact closely related to transport in media with memory as well as to transatlantic cables. This reinforces the universality of mathematical theories, and often unexpected relations can be found.

3.2 Boundary conditions

It is an interesting exercise to find appropriate boundary conditions for these models. Let us focus on the correlated random walk model (27). Since the model equations are hyperbolic, we need to look at the characteristics. For the first equation, the

characteristics are $x(t) = x+\gamma t$ and for the second equation it is $x(t) = x-\gamma t$. Hence the variable u^+ needs boundary conditions on the left boundary, while no boundary condition on the right boundary. In Figure **??** we indicate the characteristics with arrows. Formally, we define the domain boundary of $\Omega = [0, l] \times [0, t)$ as *hyperbolic boundary*

$$\partial\Omega = \partial\Omega^+ \cup \partial\Omega^-$$

with

$$\partial\Omega^+ := \{0\} \times [0, t) \cup [0, l] \times \{0\}, \qquad \partial\Omega^- := [0, l] \times \{0\} \cup \{L\} \times [0, t).$$

Then u^+ needs boundary conditions at $\partial\Omega^+$ and u^- needs boundary conditions at $\partial\Omega^-$. Both quantities require initial conditions:

$$u^+(x, 0) = u_0^+(x), \qquad u^-(x, 0) = u_0^-(x).$$

Homogeneous Dirichlet boundary conditions take the form

$$u^+(0, t) = 0, \qquad u^-(l, t) = 0,$$

while homogeneous Neumann boundary conditions are

$$u^+(0, t) = u^-(0, t), \qquad u^-(l, t) = u^+(l, t).$$

Periodic boundary conditions are as expected

$$u^+(0, t) = u^+(l, t), \qquad u^-(l, t) = u^-(0, t).$$

The corresponding initial-boundary value problems for the correlated random walk as well as for the Cataneo equations and for the telegraph equation have been studied in great detail in [15], including results on existence, uniqueness, and positivity. One curious result is the fact that the Dirichlet problem regularizes, while the Neumann and periodic problems do not regularize.

In the next section we apply the idea of a correlated random walk to chemotaxis.

3.3 Abstract formulation

The main part of this manuscript provides analysis of a generalization of the one-dimensional correlated random walk to higher dimensions. We will construct an abstract framework of function spaces and turning operators, and the one dimensional model will arise a special case. To prepare this relation, we now formulate

equation (27) as a differential equation in a Banach space. In fact, we use the (equivalent) system (28) and introduce an *integral operator* $\mathcal{T}$ for the last term on the right hand sides:

$$\mathcal{T} : \mathbb{R}^2 \to \mathbb{R}; \qquad \begin{pmatrix} u^+ \\ u^- \end{pmatrix} \mapsto \frac{1}{2}(u^+ + u^-).$$

Here it does not look like an integral operator, but the higher dimensional version will include an integration. In fact here the integration is over the discrete space $V = \{+\gamma, -\gamma\}$. The operator norm of this linear operator can be easily computed to be

$$\|\mathcal{T}\|_1 = \frac{1}{2}.$$

It will be important later that this norm is less or equal 1. The whole right hand side of the system (28) defines another operator, which we call the *turning operator* $\mathcal{L}$:

$$\mathcal{L} : \mathbb{R}^2 \to \mathbb{R}^2; \qquad \begin{pmatrix} u^+ \\ u^- \end{pmatrix} \mapsto \begin{pmatrix} -\mu u^+ + \mathcal{T}(u^+, u^-) \\ -\mu u^- + \mathcal{T}(u^+, u^-) \end{pmatrix}.$$

If we write $\mathcal{L}$ as a matrix

$$\mathcal{L} = \frac{\mu}{2} \begin{pmatrix} -1 & 1 \\ 1 & -1 \end{pmatrix}$$

we obtain eigenvalues of $\lambda_1 = 0$ and $\lambda_2 = -\mu$. The zero eigenvalue corresponds to the fact that the total population size is conserved for equation (28). The corresponding eigenspace is spanned by the vector $(1, 1)^T$. Hence the kernel of $\mathcal{L}$ is given as

$$\ker\mathcal{L} = \langle \begin{pmatrix} 1 \\ 1 \end{pmatrix} \rangle.$$

The abstract formulation appears a bit staged, but this will form the framework for the multi dimensional situation.

3.4 Correlated random walk models for chemotaxis

We can also model chemotactic behaviour via a correlated random walk model. The action of the chemical signal on the movement mechanics of cells is very different in eukariotic cells versus amoeboid cells. In E. coli, for example, the chemical sensing receptors are internally coupled to the rotation mechanisms of the flagella. If the cell encounters an increasing signal concentration, it prolongs straight movement and reduces reorientations. This in effect leads to oriented movement up a signal gradient [32, 7]. In our context this corresponds to a change in turning rate μ depending on the signal strength and its gradient. Amoeboid cells, however, are moving through

tread milling of an internal actin-myosin filament mechanism. Amoeboid cells are able to detect directions of increased chemical signal and they can actively choose directions and adapt their speed. Hence in that case the turning rate as well as the speed are affected by the signal v [3]. In one dimension, the corresponding hyperbolic chemotaxis model reads

$$\begin{aligned} u_t^+ + (\gamma(v)u^+)_x &= -\mu^+(v,v_x)u^+ + \mu^-(v,v_x)u^- \\ u_t^- - (\gamma(v)u^-)_x &= \mu^+(v,v_x)u^+ - \mu^-(v,v_x)u^- \\ \tau v_t &= Dv_{xx} + \alpha(u^+ + u^-) - \beta v, \end{aligned} \tag{32}$$

where $u^\pm$ are as before, the densities of right and left moving particles respectively. The density of the chemical signal is given by $v(x,t)$, and $\gamma(v)$ and $\mu(v,v_x)$ are the density dependent speed and turning rate. Notice that here μ is used without a factor of $1/2$, so it is a turning rate (and not a rate of change of direction).

Like before we can use scaling arguments to compute a parabolic limit (see [20, 19] for details).

$$u_t = \left(A(v,v_x)u_x - \chi(v,v_x)uv_x\right)_x . \tag{33}$$

It is interesting to see how the diffusivity A and the chemotactic sensitivity χ depend on speed γ and turning rate μ. The diffusivity is

$$A(v,v_x) = \frac{\gamma^2(v)}{\mu^+(v,v_x) + \mu^-(v,v_x)} \tag{34}$$

while the chemotactic flux is

$$\chi(v,v_x)v_x = -\frac{\gamma(v)}{\mu^+(v,v_x) + \mu^-(v,v_x)} \left(\gamma'(v)v_x + (\mu^+(v,v_x) - \mu^-(v,v_x))\right). \tag{35}$$

When $\chi > 0$, we have *positive taxis*, which supports aggregation. Here we have two effects which can cause chemotactic flow:

1. If $\gamma = \gamma(v)$ and $\gamma'(v) < 0$, then particles slow down at high concentrations of v which leads to aggregation at high concentrations of v. Or, alternatively,

2. If $\mu^+ < \mu^-$ for $v_x > 0$, then the turning rate is reduced when moving up the gradient of v, which also leads to aggregation.

Specifically, we study two examples.

Example 1 (and homework): Assume γ =const and

$$\mu^{\pm}(v, v_x) = \frac{\gamma}{2A} \left(\gamma \mp \varphi(v) v_x\right)^+ .$$

1. Describe a biological situation for the above choice of μ and γ. Does this choice correspond to the bacterial or amoeboid case? Explain.

2. Compute the diffusivity A and the chemotactic flux χv_x.

Example 2: For the second example, we consider the case where $\tau = D = 0$, and $\gamma(v) = v$. We therefore have that

$$\begin{aligned} u_t^+ + (\gamma(v)u^+)_x \qquad &= u_t^+ + \left(\tfrac{\alpha}{\beta}(u^+ + u^-)u^+\right)_x \\ &= u_t^+ + \tfrac{\alpha}{\beta}\left(u^{+2}\right)_x + \tfrac{\alpha}{\beta}\left(u^+ u^-\right)_x . \end{aligned} \tag{36}$$

We see that the first two terms on the right hand side come from Burger's equation. The standard form of Burger's equation,

$$u_t + (u^2)_x = 0,$$

and it is well known that Burger's equation has shock solutions [1]. Hence in this case we might expect shock solutions for the chemotaxis model. In [19] we use the method of viscosity solutions to further analyse the appearance of sharp gradients in chemotaxis invasion waves.

4 Transport equations

Transport equations are a powerful tool to derive mesoscopic models for the spatial spread of populations. They are particulallry useful if the movement velocity (= speed · direction) of the individuals is of importance. The theory of kinetic transport equations developed from the thermodynamics of diluted gases (see e.g. [2]) and has since developed for biological populations as well. One major difference between physical and biological applications is the number of conserved quantities. While in ideal gas theory five quantities are conserved (mass, three momentum components, energy), in biological populations, we often only conserve mass. Mathematically the conserved quantities show up as linear independent functions in the kernel of a so called *turning operator*. The kernel of the turning operator in gas theory is five dimensional, while in our applications it is one dimensional. This is, in a nutshell,

the main difference between physical and biological applications. The rest is details, which we will present as fully as possible in this manuscript.

We need to distinguish two important cases. Case 1: the kernel of the turning operator contains only constant functions and case 2: the kernel is spanned by a function that depends on the velocity. Such a function is called *Maxwellian* in a physical context. The first case allows for a quite general theory as was developed in Othmer and Hillen in [16, 31], while the second case is more complicated. We use the remainder of Sections **??** and Section **??** to study case 1,where we explain the mathematical setup, derive the parabolic limit, and apply the method to chemotaxis. Case 2 is covered in Sections **??** and **??**, where we consider nonisotropic diffusion models and applications to wolf movement and brain tumor spread.

4.1 The mathematical set-up

We begin by parameterizing a population density $p(x, v, t)$ by space x, velocity v and time t. This allows us to incorporate individual cell movement into the model, an important feature which distinguishes transport models from macroscopic models. As we are typically dealing with biological phenomena, we take $t \geq 0$ and $x \in \mathbb{R}^n$, with $n = 2, 3$. The case of $n = 1$ corresponds to the one-dimensional correlated random walk, which we studied in the previous sections. The velocities v are taken from V, where $V \subset\subset \mathbb{R}^n$ and $V = [s_1, s_2] \times \mathbb{S}^{n-1}$ or $V = s\mathbb{S}^{n-1}$. The general transport equation for a population density $p(x, v, t)$ is thus

$$p_t + v \cdot \nabla p = -\mu p + \mu \int_V T(v, v')p(x, v', t)dv', \tag{37}$$

where we omitted the arguments, except in the integral. The terms on the left hand side describe the particles' movement in space, while the terms on the right hand side describe how the particles change direction. The parameter μ is the *turning rate*, which describes how often the particles change direction. As such, $\frac{1}{\mu}$ describes the mean run length, in other words, how long a particle travels on average in a straight line before it changes direction. The distribution $T(v, v')$ inside the integral is called the *turning kernel*, and describes the probability that a cell traveling in the direction of v' will turn into the direction of v. As such, the first term on the right hand side describes cells turning out of velocity v, while the integral term describes cells turning into velocity v from all other directions $v' \in V$. Together, these two terms are called the *turning operator*. Here we follow the theory as developed by Stroock [35], Othmer et al. [30] and Hillen and Othmer [16, 31].

Given the compact set V of possible velocities, we work in the function space

$L^2(V)$ and we denote by $\mathcal{K} \subset L^2(V)$ the cone of non-negative functions. Given by the right hand side of equation (37) we define an integral operator on $L^2(V); \mathcal{T} : L^2(V) \to L^2(V)$ as

$$\mathcal{T}\phi(v) = \int_V T(v, v')\phi(v')dv'$$

with adjoint

$$\mathcal{T}^*\phi(v') = \int_V T(v', v)\phi(v)dv$$

The integral kernel T and the integral operator $\mathcal{T}$ set the stage for the theory. In the context of biological applications, we make the following general assumptions. We list the assumptions right here, while we will explain them in detail right after.

Basic Assumptions:

(T1) $T(v, v') \geq 0$, $\int_V T(v, v')dv = 1$, and $\int_V \int_V T^2(v, v')dv'dv < \infty$.

(T2) There is a function $u_0 \in \mathcal{K}\backslash\{0\}$, a $\rho > 0$ and an $N > 0$ such that for all $(v, v') \in V \times V$, either

(a) $u_0(v) \leq T^N(v', v) \leq \rho u_0(v)$, or

(b) $u_0(v) \leq T^N(v, v') \leq \rho u_0(v)$,

where the N-th iterate of T is

$$T^N(v', v) = \int_V \dots \int_V T(v', w) \dots T(w_{N-1}, v)dw_1 \dots dw_{N-1}.$$

(T3) $\|\mathcal{T}\|_{\langle 1\rangle^\perp} < 1$, where $L^2(V) = \langle 1\rangle \oplus \langle 1\rangle^\perp$.

(T4) $\int_V T(v, v')dv' = 1$.

Assumption (T1): Assumption (T1) implies that $T(\cdot, v')$ is a non-negative probability density on V. The fact that $T \in L^2(V \times V)$ implies that $\mathcal{T}$ and $\mathcal{T}^*$ are Hilbert-Shmidt operators, defined as follows ([12]):

Definition 1. *An integral operator $\mathcal{T}f(v) = \int T(v, v')f(v')dv'$ with $T \in L^2(V \times V)$ is called a Hilbert-Schmidt operator.*

Hilbert-Schmidt operators have some compactness properties:

Theorem 1. *([12]) Hilbert-Schmidt operators are bounded and compact.*

Also, (T1) implies that $\mathcal{T}$ and $\mathcal{T}^*$ are positive operators.

Assumption (T2) Assumption (T2a) ensures that $\mathcal{T}^*$ is u_0-positive in the sense of Krasnosleskii [25], while (T2b) ensures that $\mathcal{T}$ is u_0-positive. One of these is sufficient. Krasnoselskii defines u_0-positivity as follows.

Definition 2. *Let X be a Banach space, $\mathcal{K}$ the non-negative cone and $L : X \to X$ linear. Then*

(a) L is positive it $L : \mathcal{K} \to \mathcal{K}$.

(b) Let L be positive. L is u_0-bounded from below if there is a fixed $u_0 \in \mathcal{K}\backslash\{0\}$ such that $\forall \phi \in \mathcal{K}\backslash\{0\}$ $\exists N > 0, \alpha > 0$ with

$$\alpha u_0 \leq L^N \phi.$$

(c) Let L be positive. L is u_0-bounded from above if there is a fixed $u_0 \in \mathcal{K}\backslash\{0\}$ such that $\forall \psi \in \mathcal{K}\backslash\{0\}$ $\exists N > 0, \beta > 0$ with

$$L^N \psi \leq \beta u_0.$$

(d) L is u_0-positive if conditions (b) and (c) are both satisfied.

(e) $\mathcal{K}$ is reproducing if for all $\phi \in X$ there exist $\phi^+, \phi^- \in \mathcal{K}$ such that $\phi = \phi^+ - \phi^-$.

Using this definition, we can prove the following Lemma:

Lemma 1. *Assumption (T2a) implies that $\mathcal{T}^*$ is u_0-positive, while (T2b) implies that $\mathcal{T}$ is u_0 positive.*

Proof. Consider $\phi \in \mathcal{K}$. We compute the iterate

$$\begin{aligned} \mathcal{T}^{*N}\phi &= \int_V T(v', w_1) \cdots T(w_{N_1}, v)\phi(v')dw_1 \ldots dw_{N+1}dv' \\ &= \int_V T^N(v', v)\phi(v')dv' \\ &\geq \int_V u_0(v)\phi(v')dv' = u_0(v)\int_V \phi(v')dv' = \alpha u_0(v). \end{aligned}$$

The last inequality is a direct consequence of (T2a). Similarly, we have

$$\mathcal{T}^{*N}\phi \leq \int_V \rho u_0(v)\phi(v')dv' = \rho \int_V \phi(v)dv u_0(v) = \beta u_0(v).$$

The second statement has a very similar proof. □

Condition (T2) has an interesting biological meaning. It is not assumed that the kernel T is positive. In fact, it is allowed for T to have support that is smaller than V, but some iterate of T must cover V. For example if individuals are able to turn for up to 60 degrees per turn, then they are able to reach any direction after 3 turns. In that case $\mathcal{T}^3$ would be u_0 positive. See Figure **??** for an illustrative explanation. Using (T2) we are more general than most of the publications on transport equations in biology. It is almost always assumed that $T > 0$, but here we can relax that assumption.

The u_0 positivity is already sufficient to have a Krein-Rutman property:

Theorem 2. *(Krasnoselskii, [25], Theorems 2.10, 2.11)*
Let K be a reproducing non-negative cone in X. Let L be u_0-positive. Let $\varphi_0 \in \mathcal{K}$ be an eigenfunction of L. Then

(i) $L\varphi_0 = \lambda_0\varphi_0$ and λ_0 is a simple, leading eigenvalue,

(ii) φ_0 is unique in $\mathcal{K}$ up to scalar multiples, and

(iii) $|\lambda_0| > |\lambda|$ for all other eigenvalues λ.

In our case we have

$$\mathcal{T}^*1 = \int_V T(v', v)1dv' = 1$$

by (T1). Hence $\varphi_0 = 1 \in \mathcal{K}$ is the leading non-negative eigenfunction of $\mathcal{T}^*$ with eigenvalue $\lambda_0 = 1$. All of the other eigenvalues are such that $|\lambda| < 1$. We also have

$$\mathcal{T}1 = \int_V T(v, v')dv' = 1$$

by (T4).This means that we also have that $\varphi_0 = 1$ is the leading non-negative eigenfunction of $\mathcal{T}$.

Assumption (T3): Note that in Krasnoselskii's theorem above it is assumed that there exists an eigenfunction in $\mathcal{K}$. This is not always the case, and assumption (T3)

ensures the existence of a spectral gap between the leading eigenvector $\varphi_0 = 1$ and the remainder of the spectrum. We will show later that if $\mathcal{T}$ is a normal operator (or if $\mathcal{T}^*$ is normal), then (T2) implies (T3).

Assumption (T4): Condition (T4) looks as natural as the second condition in (T1). It has, however a very different meaning. The meaning of (T4) is that the eigenvalue equation

$$\int_V T(v, v')\phi(v')dv' = \lambda\phi(v)$$

has a constant solution $\phi(v) = 1$ with eigenvalue $\lambda = 1$. This is a very special case that allows us to develop a full theory and to do the macroscopic scalings done later in this chapter. If the leading eigenfunction $\varphi_0(v)$ is not constant the methods will change slightly, and particular care must be given to the resulting non-isotropic diffusion equations (see Section **??**) . We will see that both cases are equally important in terms of applications.

4.2 The Turning Operator

The *turning operator* describes the whole right hand side of (37) and is given by $\mathcal{L} : L^2(V) \to L^2(V)$:

$$\mathcal{L}p(v) = -\mu p(v) + \mu\mathcal{T}p(v)$$

and its adjoint

$$\mathcal{L}^* = -\mu p(v) + \mu\mathcal{T}^* p(v).$$

We can now write down a result about the spectrum of the turning operator.

Lemma 2. *Assume (T1)-(T4). Then 0 is a simple eigenvalue of $\mathcal{L}^*$ and $\mathcal{L}$ with leading eigenfunction $\varphi_0 = 1$. All other eigenvalues λ satisfy $-2\mu < Re\lambda < 0$. All other eigenfunctions have zero mass.*

Proof. Both $\mathcal{T}$ and $\mathcal{T}^*$ have a spectral radius of 1, which implies that $\mu\mathcal{T}$ has a spectral radius of μ. We therefore have

$$-2\mu < \mathrm{Re}\lambda < 0.$$

If $\varphi \neq \varphi_0$ is another eigenfunction, then $\varphi \in \langle 1 \rangle^\perp$ which implies

$$0 = \int_V \varphi(v) 1 dv = \int_V \varphi(v) dv.$$

□

Condition (T3) allows us to introduce another constant, called μ_2, which will give us information about the dissipativity of the turning operator. Consider $\psi \in \langle 1 \rangle^\perp$ then

$$\begin{aligned} \int_V \psi \mathcal{L} \psi dv &= -\mu \int_V \psi^2 dv + \mu \int_V \psi \mathcal{T} \psi dv \\ &\leq -\mu(1 - \|\mathcal{T}\|_{\langle 1 \rangle^\perp}) \int_V \psi^2 dv \\ &= -\mu_2 \|\psi\|_2^2 \end{aligned}$$

with $\mu_2 = \mu(1 - \|\mathcal{T}\|_{\langle 1 \rangle^\perp})$ and $\|\mathcal{T}\|_{\langle 1 \rangle^\perp} < 1$.

4.3 Normal operators

In this section we discuss what it means for an operator to be normal, and explore some of the consequences of this characteristic.

Definition 3. *An operator A is defined to be normal if $AA^* = A^*A$.*

Theorem 3. *If A is normal, then there exists a complete orthogonal set of eigenfunctions. A has a spectral representation $A = \sum \lambda_j P_j$ where λ_j are the eigenvalues and P_j the spectral projections.*

If $\mathcal{T}$ is normal, then we can choose an orthonormal basis φ_n with $\|\varphi_n\| = 1$.

Lemma 3. *If $\mathcal{T}$ is normal, then (T3) follows from (T1) and (T2).*

Proof. Consider the operator norm of $\mathcal{T}$ on $\langle 1\rangle^{\perp}$:

$$\begin{aligned}
\|\mathcal{T}\|_{\langle 1\rangle^{\perp}} &= \sup_{\substack{\phi\in\langle 1\rangle^{\perp}\\ \|\phi\|_2=1}} \|\mathcal{T}\phi\|_2 \\
&= \sup_{\phi} \|\mathcal{T}\sum_{n=1}^{\infty}\alpha_n\phi_n\|_2 \\
&= \sup_{\phi} \|\sum_{n=2}^{\infty}\alpha_n\lambda_n\phi_n\|_2 \\
&= \sup_{\phi} \left(\sum_{n=2}^{\infty}|\alpha_n\lambda_n|^2\right)^{\frac{1}{2}} \\
&< \sup_{\phi} \left(\sum_{n=2}^{\infty}|\alpha_n|^2\right)^{\frac{1}{2}} = \|\phi\|_2 = 1.
\end{aligned}$$

□

In our case we need to check if $\mathcal{T}$ is normal:

$$\begin{aligned}
\mathcal{T}\mathcal{T}^*\phi &= \mathcal{T}\left(\int_V T(v,v')\phi(v')dv'\right) \\
&= \int_V\int_V T(v,v'')T(v',v'')\phi(v')dv'dv'' \\
\mathcal{T}^*\mathcal{T}\phi &= \int_V\int_V T(v'',v)T(v'',v')\phi(v')dv'dv''.
\end{aligned}$$

In order for our operator to be normal, we thus obtain the necessary symmetry condition

$$\int_V T(v,v'')T(v',v'')dv'' = \int_V T(v'',v)T(v'',v')dv''.$$

This is satisfied, for example, when T is a symmetric kernel of the form $T(v,v') = T(v',v), \forall (v,v')\in V^2$.

4.4 Important Examples

We now consider two important examples, and investigate how the theory discussed so far above applies.

4.4.1 Example 1: Pearson walk

For the first example, we will choose our space of directions to be a sphere of constant radius, i.e. $V = s\mathbb{S}^{n-1}$. This means that our particles can choose any direction, and will travel with constant speed. We will choose the simplest turning kernel, which is constant and normalized: $T(v, v') = \frac{1}{|V|}$.

We will now check (using ✓) if our four basic assumptions are satisfied for this simple choice of V and T, which in turn allows us to apply any of the theory that we develop later.

(T1) $T \geq 0$ ✓, $\int_V T dv = 1$ ✓, $\int_V \int_V T^2 dv dv' = 1$ ✓, and so the conditions of assumption (T1) are met.

(T2) Not only do we have that $T \geq 0$, but we actually have the stronger condition $T > 0$. This implies that $\mathcal{T}$ is u_0-positive.

(T3)

$$\mathcal{T}^*\phi = \int_V \frac{1}{|V|}\phi(v')dv' = \mathcal{T}\phi = \int_V \frac{1}{|V|}\phi(v)dv$$

We can thus conclude that $\mathcal{T}$ is self adjoint and henceforth it is normal. Then by Lemma 3, we can conclude that (T3) is satisfied. ✓

(T4) $\int_V T dv' = 1$. ✓

The Pearson walk satisfies all assumptions (T1)-(T4), and it will form our prototype for the theory and scaling developed later.

4.4.2 Example 2: movement on fibre networks

There are many examples which arise naturally in biology where the particles in question, whether they be animals or cells, make their turning decisions based on their environment. For example, glioma cells diffusing in the brain will use the white matter tracts as highways for their movement [5, 10, 9, 38]. We also see this phenomenon in ecology, where wolves will use paths that are cut in the forest for oil exploration to hunt more efficiently [26, 27]. We thus consider in this example these types of situations, where our turning kernel is is given by an underlying anisotropy of the environment. We use unit vectors $\theta \in \mathbb{S}^{n-1}$ to describe the anisotropies of the environment through a directional distribution $q(x, \theta)$ with

$$\int_{\mathbb{S}^{n-1}} q(x, \theta)d\theta \quad \text{and} \quad q(x, \theta) > 0.$$

In the context of glioma growth, $q(x,\theta)$ denotes the distribution of nerve fibre directions in each location x. In the example of wolf movement the function q would provide information of preferred movement directions due to roads or seismic lines. We discuss these two examples later in Section **??** and **??**. We assume that individuals favour directions that are given by the environment, and, for simplicity, we consider unit speed $|v| = 1, V = \mathbb{S}^{n-1}$. Then $T(v,v',x) = q(x,v)$. The assumption (T1)-(T4) relate to the v dependence only, hence in the following we ignore the x dependence in q, noting, however, that q, in general, would depend on x.

(T1) $q \geq 0$ ✓, $\int_V T(v,v')dv = \int_V q(v)dv = 1$, ✓and $\int_V \int_V q^2(v)dvdv' = |V| \cdot \int_V q^2(v)dv < \infty$, henceforth $q \in L^2(\mathbb{S}^{n-1})$. ✓

(T2) We first compute the iterates:

$$\begin{aligned} T^N(v',v) &= \int_V \cdots \int_V T(v',w_1)\cdots T(w_{N-1}v)dw_1\cdots dw_{N-1} \\ &= \int_V \cdots \int_V q(v')q(w_1)\cdots q(w_{N-1})dw_1\cdots dw_{N-1} \\ &= q(v') \end{aligned}$$

Hence condition (T2a) becomes:

$$u_0(v) \leq q(v') \leq \rho u_0(v),$$

which is satisfied only if $q > 0$.

The condition (T2b) becomes:

$$u_0(v) \leq q(v) \leq \rho u_0(v),$$

and so we have a weaker condition, only requiring that q to be u_0 positive.

(T3) Is $\mathcal{T}$ normal? $\mathcal{T}$ would be normal if

$$\int_V q(v)q(v')dv'' = \int_V q(v'')q(v'')dv''$$

which is equivalent to

$$|V|q(v)q(v') = \|q\|_2^2$$

and we see that this is true if q =const., which brings us back to the Pearson case. So in general, $T(v,v') = q(v)$ is not normal. Therefore we must do some more work in order to verify (T3) and we compute $\|\mathcal{T}\|_{\langle 1\rangle^\perp}$ directly

$$\begin{aligned}\|\mathcal{T}\|_{\langle 1\rangle^\perp} &= \sup_{\substack{\phi\in\langle 1\rangle^\perp\\ \|\phi\|=1}} \left|\left|\int_V q(v)\phi(v')dv'\right|\right| \\ &= \sup \left|\left| q(v)\int_V \phi(v')dv'\right|\right| \\ &= 0.\end{aligned}$$

Hence on $\langle 1\rangle^\perp$ the operator $\mathcal{T}$ is the zero operator. Which satisfies assumption (T3), but it also shows that the splitting of $L^2(V) = \langle 1\rangle \oplus \langle 1\rangle^\perp$ is not a good choice here. Indeed, we will later see that we should choose $L^2(V) = \langle q\rangle \oplus \langle q\rangle^\perp$.

(T4) Finally, we check condition (T4).

$$\int_V T(v,v')dv' = q(v)|V| = 1,$$

which is only true for $q(v)$ =const.

So for this example, if $T(v,v') = q(v)$ is not constant, then it fails (T4) and possibly (T3).

4.4.3 Example 3 (homeork) Symmetric kernels

Check if symmetric kernels of the form a), b) or c) satisfy the assumptions (T1)-(T4):

$$\begin{aligned} a) &\qquad T(v,v') = t(|v-v'|) \\ b) &\qquad T(v,v') = t(v-v') \\ c) &\qquad T(v,v') = t(v')\end{aligned}$$

4.5 Main Spectral Result

In this section, we summarize the results thus far into one main theorem and provide a proof of the missing pieces.

Theorem 4. *[16] Assume (T1)-(T4). Then*

1) 0 is a simple leading eigenvalue of $\mathcal{L}$ with unique eigenfunction $\varphi_0 = 1$,

2) All other eigenvalues λ are such that $-2\mu < Re\lambda \leq -\mu_2 < 0$ and all other eigenfunctions have zero mass.

3) $L^2(V) = \langle 1 \rangle \oplus \langle 1 \rangle^\perp$ *and for all* $\psi \in \langle 1 \rangle^\perp$*:*

$$\int_V \psi \mathcal{L} \psi dv \leq -\mu_2 \|\psi\|_2^2, \quad \text{where} \quad \mu_2 = \mu\Big(1 - \|\mathcal{T}\|_{\langle 1 \rangle^\perp}\Big),$$

4) The $\|\mathcal{L}\|$ *has a lower and upper estimate*

$$\mu_2 \leq \|\mathcal{L}\|_{\mathcal{L}(L^2(V), L^2(V))} \leq 2\mu,$$

5) $\mathcal{L}_{\langle 1 \rangle^\perp}$ *has a linear inverse* $\mathcal{F}$ *(pseudo-inverse) with*

$$\frac{1}{2\mu} \leq \|\mathcal{F}\|_{\langle 1 \rangle^\perp} \leq \frac{1}{\mu_2}.$$

Proof. We have already verified parts 1)–3) earlier in this section, thus we now prove 4) and 5). To verify 4):

$$\begin{aligned}
\|\mathcal{L}\|_{\mathcal{L}(L^2(V), L^2(V))} &= \sup_{\substack{\phi \in L^2(V) \\ \|\phi\| = 1}} \|\mathcal{L}\phi\|_2 \\
&\leq \sup_{\phi = \alpha + \phi^\perp} \left(\underbrace{\|\mathcal{L}\alpha\|_2}_{=0} + \|\mathcal{L}\phi^\perp\|_2 \right) \\
&= \sup_{\phi^\perp \in \langle 1 \rangle^\perp} \|\mathcal{L}\phi^\perp\|_2 \\
&= \sup_{\phi^\perp \in \langle 1 \rangle^\perp} \| - \mu\phi^\perp + \mu\mathcal{T}\phi^\perp\|_2 \\
&\leq \sup_{\phi \in \langle 1 \rangle^\perp} \mu\|\phi^\perp\|_2 + \mu\|\mathcal{T}\phi^\perp\|_2 \\
&\leq \sup_{\phi^\perp \in \langle 1 \rangle^\perp} 2\mu\|\phi^\perp\|_2
\end{aligned}$$

and $\forall \phi \in \langle 1 \rangle^\perp$, $\|\phi\|_2 = 1$ we have

$$\mu_2 \|\phi\|_2^2 \leq -\int \phi \mathcal{L} \phi dv \underset{\text{Hölder}}{\leq} \|\phi\|_2 \cdot \|\mathcal{L}\phi\|_2 \leq \|\mathcal{L}\|_{\mathcal{L}(L^2(V), L^2(V))},$$

which implies $\mu_2 \leq \|\mathcal{L}\| \leq 2\mu$.

Part 5) follows directly from $\mathcal{F} = \big(\mathcal{L}|_{\langle 1 \rangle^\perp}\big)^{-1}$. For example, if $\mathcal{F}\phi = z$ and $\phi, z \in \langle 1 \rangle^\perp$, then $\mathcal{L}z = \phi$ and

$$
\begin{aligned}
&\|\phi\| = \|\mathcal{L}z\| \\
\Rightarrow\quad & \mu_2\|z\| \leq \|\phi\| \leq 2\mu\|z\| \\
\Rightarrow\quad & \frac{1}{2\mu}\|\phi\| \leq \|z\| \leq \frac{1}{\mu_2}\|\phi\| \\
\Rightarrow\quad & \frac{1}{2\mu}\|\phi\| \leq \|\mathcal{F}\phi\| \leq \frac{1}{\mu_2}\|\phi\|
\end{aligned}
$$

□

4.6 Existence and uniqueness

Since the transport equation as formulated in (37) is linear, we immediately get existence and uniqueness of solutions as follows. We denote the shift operator $A := -(v \cdot \nabla)$ with domain of definition

$$D(A) = \{\phi \in L^2(\mathbb{R}^n \times V) : \phi(., v) \in H^1(\mathbb{R}^n)\}.$$

The shift operator is skew-adjoint and, according to Stones theorem ([4, 34]) it generates a strongly continuous unitary group on $L^2(\mathbb{R}^n \times V)$. The right hand side of (37) is given by the bounded operator $\mathcal{L}$, hence it is a bounded perturbation of the shift group. Consequently, also (37) generates a strongly continuous solution group on $L^2(\mathbb{R}^n \times V)$. Moreover. given initial conditions $u_0 \in D(A)$, then a unique global solution exists in

$$C^1([0, \infty), L^2(\mathbb{R}^n \times V)) \cap C([0, \infty), D(A)).$$

5 The formal diffusion limit

The computation of the diffusion limit, as presented here, is one of the standard methods for the analysis of transport equations. The equation type of a transport equation is hyperbolic, as it is based on pieces of balistic motion, interspersed with directional changes. As the frequency of these changes becomes large, and the speed is large, then the movement looks, on a macroscopic scale like diffusion (see Figure **??**). Mathematically, this macroscopic limit can be obtained via a formal asymptotic expansion with a small parameter ε. This parameter ε related the microscopic spatial scale to a macroscopic spatial scale. We will see that the above assumptions (T1)-(T4) allow us to obtain a well defined and uniformly parabolic limit equation, where the diffusivity is given by the turning kernel T. Before we present the scaling method in Section 5.2, we discuss realistic scaling arguments for E. coli bacteria.

5.1 Scalings

INSERT FIGURE HERE

We now consider E. coli bacteria as an example of different time and spatial scales.
Turning: E. coli turn about once per second. Hence the turning rate μ satisfies $\frac{1}{\mu} \sim \frac{1}{s}$. From the point of view of the cell, we call this the time-1 timescale of $\tau_{\text{turn}} = \mathcal{O}(1)$,
Drift: If observed over 50-100 turns, the trajectories appear directed, and a net displacement can easily be measured. We call this the intermediate drift time scale $\tau_{\text{drift}} \sim \mathcal{O}\left(\frac{1}{\varepsilon}\right)$, and $\varepsilon \sim 10^{-2}$.
Diffusion: If we allow for 2500-10000 turns, then the trajectories look like diffusion and random movement. Hence we introduce a third time scale of $\tau_{\text{diff}} \sim \mathcal{O}\left(\frac{1}{\varepsilon^2}\right)$.

A common first step in biological problems is to perform a nondimensionalization. This serves to remove dimension from the problem, thus simplifying the model. In many situations, this will also reduce the number of parameters which we are dealing with, and it often allows us to identify large and small parameter combinations. In the case of transport equations, as introduced in the previous section, we introduce

- $\tilde{v} = \frac{v}{s}$: where s is the characteristic speed. In case of E. coli it is about 10-20 $\frac{\mu\text{m}}{\text{s}}$,
- $\tilde{x} = \frac{x}{L}$: where L is the characteristic length scale. For E. coli bacterial colonies are of the order of 1mm-1cm, and
- $\tilde{t} = \frac{t}{\sigma}$: where σ is the macroscopic time scale of observation. In the bacterial case it is about 1-10h.

If we apply these scalings, then the transport equation becomes

$$\frac{1}{\sigma}\frac{\partial p}{\partial \tilde{t}} + \frac{s}{L}\tilde{v} \cdot \nabla_{\tilde{x}} p = -\mu p + \mu \int_V T p dv'.$$

Using the values which we identified for E. coli, we find

$$\sigma \approx 1 - 10 \text{ hours } = 3600 - 36000 \text{ seconds } \sim 10^4 s,$$

and

$$\frac{s}{L} \approx \frac{10\frac{\mu \mathrm{m}}{\mathrm{s}}}{10^{-3}\mathrm{m}} = \frac{10 \cdot 10^{-6}\frac{\mathrm{m}}{\mathrm{s}}}{10^{-3}\mathrm{m}} = 10^{-2}\frac{1}{\mathrm{s}}.$$

When $\varepsilon = 10^{-2}$, we then have $\frac{1}{\sigma} \sim \varepsilon^2$ and $\frac{s}{L} \sim \varepsilon$. If we remove the $\sim$, then we obtain the resulting scaled transport equation:

$$\varepsilon^2 p_t + \varepsilon v \cdot \nabla p = \mathcal{L} p. \tag{38}$$

5.2 The formal diffusion limit

To compute the formal diffusion limit, we will begin by studying a regular perturbation, or Hilbert expansion of p with respect to ε. This gives us

$$p(x, v, t) = p_0(x, v, t) + \varepsilon p_1(x, v, t) + \varepsilon^2 p_2(x, v, t) + h.o.t. \tag{39}$$

We will begin by substituting this expansion into equation into 38 and match orders of ε.

Order ε^0:

$$\mathcal{L} p_0 = 0,$$

which implies that p_0 is in the kernel of $\mathcal{L}$, hence

$$p_0(t, x, v) = \bar{p}(x, t),$$

which is independent of v.

Order ε^1:

$$v \cdot \nabla p_0 = \mathcal{L} p_1. \tag{40}$$

This equation can be solved for p_1 if $v \cdot \nabla p_0 \in \langle 1 \rangle^{\perp}$, so we need to check if this solvability condition is satisfied. Computing the following inner product of $v \cdot \nabla p_0$ and 1 we find:

$$\int_V v \cdot \nabla p_0 1 dv = \nabla \left(\underbrace{\int_V v dv}_{\substack{=0 \text{ due to} \\ \text{symmetry of } V}} \quad \bar{p} \right) = 0.$$

Hence equation (40) can be solved as $p_1 = \mathcal{F}(v \cdot \nabla p_0) = \mathcal{F}(v \cdot \nabla \bar{p}_0)$,

Order ε^2:

$$p_{0t} + v \cdot \nabla p_1 = \mathcal{L} p_2. \tag{41}$$

Which is a bit more complicated to solve than the first two cases. Here we have two options for how to proceed; a) integrate, or b) use the solvability condition. In the case studied here, a) and b) are equivalent, however, in other cases we would integrate.

If we integrate equation (41), we obtain

$$\int_V p_{0t} + v \cdot \nabla p_1 dv = 0,$$

since the right hand side integrates to 0. Plugging in the results from the order 0 and order 1 matching, this becomes

$$\int_V \bar{p}_t(x,t) dv + \int_V v \cdot \nabla \mathcal{F}(v \cdot \nabla \bar{p}(x,t)) dv = 0.$$

Since $\bar{p}_t$ does not depend on v, we can simplify the first term. Also, since ∇ is a spatial derivative, and the integral is over the velocity space, we can take the derivative out of the integral in the second term. This equation thus becomes

$$|V| \bar{p}_t(x,t) + \nabla \cdot \int_V v \mathcal{F} v dv \cdot \nabla \bar{p}(x,t).$$

We can simplify this to

$$\bar{p}_t = \nabla \cdot D \nabla \bar{p} \tag{42}$$

where the diffusion tensor D is defined to be

$$D = -\frac{1}{|V|} \int_V v \mathcal{F} v^{\perp} dv = -\frac{1}{|V|} \int_V v \otimes \mathcal{F} v dv.$$

Where we use two equivalent forms to denot an exterior product. We can write this in index notation as well

$$\nabla \cdot D \nabla = \sum_{i,j=1}^{n} \partial_i D^{ij} \partial_j, \quad \text{with} \quad D^{ij} = \frac{1}{|V|} \int_V v^i \mathcal{F} v^j dv.$$

5.2.1 Example: Pearson Walk

We can once again consider the Pearson walk as an example. Recall from before that for this example we choose $V = s\mathbb{S}^{n-1}$ and $T(v, v') = \frac{1}{|V|}$. We first must compute the inverse function $\mathcal{F}$. Given $\phi \in \langle 1 \rangle^{\perp}$, we wish to find $z \in \langle 1 \rangle^{\perp}$ such that $\mathcal{L}z = \phi$. We will find it useful to use the fact that

$$z \in \langle 1 \rangle^{\perp} \Rightarrow \int_V z(v)dv = 0.$$

Now if we apply the operator $\mathcal{L}$, we have that $\mathcal{L}z = \phi$ is equivalent with

$$-\mu z(v) + \mu \underbrace{\int_V \frac{1}{|V|} z(v')dv'}_{=0} = \phi(v),$$

and so $z(v) = -\frac{1}{\mu}\phi(v)$. Hence

$$\mathcal{F} = -\frac{1}{\mu} \quad \text{as multiplication operator.}$$

Then for this example, we find that the diffusion tensor is

$$D = \frac{1}{\mu|V|} \int_V vv^{\mathrm{T}} dv.$$

In order to have an explicit form for D, we must then compute

$$\int_V vv^{\mathrm{T}} dv, \quad \text{with} \quad V = s\mathbb{S}^{n-1}.$$

For example, in 2-dimensions: $V = s\mathbb{S}^1$, and $v = s\begin{pmatrix}\cos\phi \\ \sin\phi\end{pmatrix}$. We can then explicitly compute

$$vv^{\mathrm{T}} = s^2 \begin{pmatrix} \cos^2\phi & \cos\phi\sin\phi \\ \cos\phi\sin\phi & \sin^2\phi \end{pmatrix},$$

and so

$$D = \frac{s^2}{|V|} \int_0^{2\pi} \begin{pmatrix} \cos^2\phi & \cos\phi\sin\phi \\ \cos\phi\sin\phi & \sin^2\phi \end{pmatrix} sd\phi.$$

We can then solve by integrating component wise. If we consider this tensor in 3 dimensions, then we have double integrals of trigonometric functions to solve. This

is still possible, but tedious. But then in higher dimensions the integral becomes more and more cumbersome. In the proof of the next Lemma we propose a clever use of the divergence theorem to compute the above integral in any dimension. As shown by Hillen in [13], this method can be generalized to higher dimensions and higher velocity moments.

Lemma 4. *Let $V = s\mathbb{S}^{n-1}, \omega_0 = |\mathbb{S}^{n-1}|$, then $|V| = s^{n-1}\omega_0$ and*

$$\int_V vv^T dv = \frac{\omega_0 s^{n+1}}{n}\mathbb{I},$$

where $\mathbb{I}$ is the n-dimensional identity matrix.

Proof. Since $\int_V vv^{\mathrm{T}} dv$ is a tensor, we use two test vectors $a, b \in \mathbb{R}^n$ and use tensor notation, i.e. summation over repeated indices

$$a_i b_i = \sum_{i=1}^{n} a_i b_i$$

then

$$\begin{aligned} a^T \int_V vv^{\mathrm{T}} dv\, b &= \int_V a_i v_i v_j b_j dv \\ &= s\int_V \frac{v_i}{|v|}(a_i v_j b_j) dv \\ &\underbrace{=}_{\substack{\text{divergence}\\ \text{theorem}}} s\int_{B_s(0)} \mathrm{div}_{v_i}(a_i v_j b_j) dv \\ &= s\int_{B_s(0)} a_i b_i dv \\ &= s|B_s(0)| a_i b_i \end{aligned}$$

We can compute $|B_s(0)|$ as follows

$$|B_s(0)| = s^n |B_1(0)| = s^n \int_{B_1(0)} dv = \frac{s^n}{n}\int_{B_1(0)} \mathrm{div}_v v dv$$

and if we apply the divergence theorem again this becomes

$$\frac{s^n}{n}\int_{\mathbb{S}^{n-1}} \sigma\cdot\sigma d\sigma = \frac{s^n}{n}|\mathbb{S}^{n-1}| = \frac{s^n}{n}\omega_0.$$

Then

$$a^{\mathrm{T}}\int_V vv^{\mathrm{T}}dv\; b = a^T\frac{s^n}{n}|\mathbb{S}^{n-1}|b = \frac{s^{n+1}}{n}\omega_0 a^{\mathrm{T}}b$$

for all vectors $a, b \in \mathbb{R}^n$. Hence

$$\int_V vv^{\mathrm{T}}dv = \frac{\omega_0 s^{n+1}}{n}\mathbb{I}.$$

□

Remarks:

1. For general symmetric V, there exists $\kappa > 0$ such that $\int_V vv^{\mathrm{T}}dv = \kappa\mathbb{I}$.

2. In [13] explicit formulas for all higher velocity moments $\int_V v_i v_j \cdots v_k dv$ were computed explicitly for any order.

Now returning to our discussion of the Pearson walk example. We can explicitly compute the diffusion tensor using the above discussion, i.e.

$$D = \frac{1}{\mu|V|}\int_V vv^{\mathrm{T}}dv = \frac{1}{\mu|V|}\frac{\omega_0 s^{n+1}}{n}\mathbb{I},$$

and since $|V| = s^{n-1}\omega_0$, this simplifies to

$$D = \frac{s^2}{\mu n}\mathbb{I}.$$

This diffusion tensor corresponds to isotropic diffusion, and so the use of the tensor is not necessary, and we can simply use a diffusion coefficient. This gives the isotropic diffusion equation

$$\bar{p}_t = \frac{s^2}{\mu n}\nabla\bar{p}.$$

5.3 Structure of the diffusion tensor

The above limit construction leads to a diffusion-like equation (42) and the first question is the question under which condition is the operator $\nabla \cdot D\nabla$ uniformly parabolic. We will see that here the condition (T3) and the corresponding constant μ_2 are important.

Lemma 5. *Assume (T1)-(T4). The diffusion tensor D is uniformly elliptic, i.e.*

$$\exists \kappa > 0 \text{ such that } \varphi \cdot D\varphi \geq \kappa |\varphi|^2.$$

Proof. Let $\varphi \in \mathbb{R}^n$ and compute

$$\varphi \cdot D\varphi = -\frac{1}{|V|} \int_V (\varphi \cdot v) \mathcal{F}(\varphi \cdot v) dv.$$

Since $\varphi \cdot v \in \langle 1 \rangle^\perp$, we can apply $\mathcal{F}$ i.e. there exists $z = \mathcal{F}(\varphi \cdot v)$ and $\mathcal{L}z = \varphi \cdot v$. Then

$$\begin{aligned} \varphi \cdot D\varphi &= -\frac{1}{|V|} \int_V \mathcal{L}z(v) z(v) dv \\ &\geq \frac{\mu_2}{|V|} \|z(v)\|_2^2 \text{ from our spectral result} \\ &= \frac{\mu_2}{|V|} \int_V \left| \mathcal{F}\left(\frac{\varphi}{|\varphi|} \cdot v \right) \right|^2 dv |\varphi|^2 \\ &\geq c_0 \frac{\mu_2}{|v|} |\varphi|^2 \end{aligned}$$

with

$$c_0 = \min_{|\varphi|=1} \int_V |\mathcal{F}(\varphi \cdot v)|^2 dv > 0.$$

Note that indeed $c_0 > 0$ since $\|\mathcal{F}\|_{\langle 1 \rangle^\perp} > \frac{1}{2\mu}$. Furthermore, the integral $\int_V |\mathcal{F}(\varphi \cdot v)|^2 dv$ does not depend on the choice of φ, since V is symmetric.

□

Theorem 5. *Assume (T1)-(T4). The differential operator $\nabla \cdot D\nabla$ generates an analytic semigroup on $L^2(\mathbb{R}^n)$. For $p(0, ., v) \in L^2(\mathbb{R}^n)$ and $\bar{p}_0(x) = \int p(0, x, v) dv$ there exists a unique global solution $\bar{p}(x, t)$ of*

$$\bar{p}_t = \nabla \cdot D\nabla \bar{p}$$

with the following properties:

$$
\begin{aligned}
&(i) && \bar{p} \in C([0,\infty), L^2(\mathbb{R}^n)) \\
&(ii) && \frac{\partial \bar{p}}{\partial t} \in C^\infty((0,\infty)\times\mathbb{R}^n) \\
&(iii) && \|\bar{p}(.,t)\|_\infty \textit{is a decreasing function of } t.
\end{aligned}
$$

Corollary 1. *(Regularity, [37]) For each $m \in \mathbb{N}$ and each $0 < \vartheta < \infty$ there exists a constant $C_0 = C_0(m, \vartheta, \|\bar{p}_0(.,t)\|_2)$such that*

$$\|\bar{p}\|_{C^m((\vartheta,\infty)\times\mathbb{R}^n)} \leq C_0.$$

5.4 Graphical Representations of the Diffusion Tensor

There are two intuitive ways to graphically represent a diffusion tensor: ellipsoids and peanuts. Let D denote a three dimensional diffusion tensor.

1. The fundamental solution of the diffusion equation in $\mathbb{R}^n$ is the multidimensional Gaussian distribution, of the form

   $$G(x,\tilde{x}) = C\exp\Big(-(x-\tilde{x})^T D^{-1}(x-\tilde{x})\Big).$$

   with an appropriate normalization constant C. This function describes the probability density of finding a random walker at a distance $w = x - \tilde{x}$ from a starting point $\tilde{x}$. Hence the level sets of $w^T D^{-1} w$ describe locations of equal probability, which is the *diffusion ellipsoid*:

   $$\mathcal{E}_c := \{w \in \mathbb{R}^n : w^T D^{-1} w = c\}$$

   The value of the constant is not important, and it is often chosen to be $c = 1$.

2. The function from $S^{n-1} \to \mathbb{R}$ defined as $\theta \mapsto \theta^T D\theta$ gives the *apparent diffusion coefficient in direction θ*, and also the *mean squared displacement in that direction*and it is called the *peanut*.

These objects are, in fact not the same. While the probability level sets are ellipsoids, the apparent diffusion coefficient is typically peanut shaped, as can be seen for our examples in Figure 6.

We chose examples of diffusion tensors in diagonal form. If they are not in diagonal form, then the ellipsoids or peanuts are rotated relative to the coordinate axis. The diffusion ellipsoid for a diagonal diffusion matrix $D = \mathrm{diag}(\lambda_1, \lambda_2, \lambda_3)$ is

$$\mathcal{E}_1 = \left\{ w \in \mathbb{R}^n : \left(\frac{w_1}{\sqrt{\lambda_1}}\right)^2 + \left(\frac{w_2}{\sqrt{\lambda_2}}\right)^2 + \left(\frac{w_3}{\sqrt{\lambda_3}}\right)^2 = 1 \right\},$$

which is clearly an ellipsoid. The peanut in this case is the map

$$\theta \mapsto \lambda_1\theta_1^2 + \lambda_2\theta_2^2 + \lambda_3\theta_3^2.$$

In Figure 6 we consider

$$D_1 := \begin{pmatrix} 5 & 0 & 0 \\ 0 & 3 & 0 \\ 0 & 0 & 1 \end{pmatrix}, \qquad D_2 = \begin{pmatrix} 8 & 0 & 0 \\ 0 & 1 & 0 \\ 0 & 0 & 0.2 \end{pmatrix}.$$

Having peanuts and ellipsoids, there is a nice way to visualize the condition of ellipticity of D.

Definition 4. *D is uniformly elliptic, if there exists a constant $\kappa > 0$ such that*

$$\theta^T \cdot D\theta > \kappa|\theta|^2, \tag{43}$$

for all vectors $\theta \in \mathbb{R}^n$.

Lemma 6. *1. The diffusion tensor D is uniformly elliptic, iff the peanut of D contains a ball.*

2. The diffusion tensor D is uniformly elliptic, iff the ellipsoid of D contains a ball.

Proof. Let us consider the peanut case first. The map $\theta \to \kappa|\theta|^2$ can be written as $\theta \to \kappa\theta^T I\theta$ with the identity matrix I. Hence it is also a peanut. A very special peanut, in fact, since it is a ball of radius κ. Then condition (43) says that the peanut of D contains the peanut of κI.

Related to the diffusion ellipsoid, we need to work a little more.

"$\Longrightarrow$" Assume D is uniformly elliptic, and consider v with $v^T D^{-1} v = 1$. Without restriction, we can study the level set of level 1. We claim:

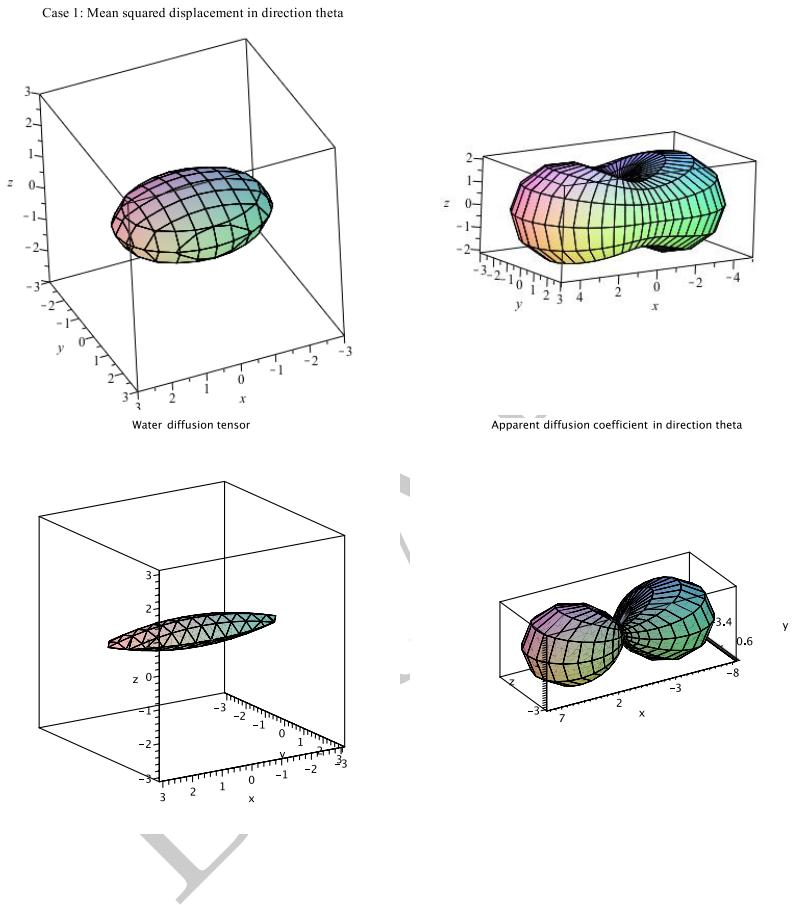

Figure 6: Left: Diffusion ellipsoid. Right: The corresponding peanut for the apparent diffusion in direction θ. Top row: example D_1, bottom row, example D_2.

Claim 1: $|v| > \sqrt{\kappa}$.
To prove Claim 1. we need to show two more statements:

Claim 2: $\inf_{|\phi|=1} \|D\phi\| \geq \kappa$**.**
Assume Claim 2 is not true. Then there exists ϕ_0 with $|\phi_0| = 1$ such that $\|D\phi_0\| < \kappa$. However,

$$\kappa = \kappa|\phi_0|^2 \leq \phi_0 D\phi_0 \leq |\phi_0|\|D\phi_0\| < \kappa,$$

which is a contradiction. Hence Claim 2 is true.

Claim 3: $\|D^{-1}\|_{op} \leq \frac{1}{\kappa}$.
Claim 2 implies that $\kappa\|\phi\| \leq \|D\phi\|$, for all $\phi \in \mathbb{R}^n$. Let $z := D\phi$, such that $\phi = D^{-1}z$. Then

$$\kappa\|D^{-1}z\| \leq \|z\| \quad \Longrightarrow \quad \frac{\|D^{-1}z\|}{|z|} \leq \frac{1}{\kappa}.$$

Hence Claim 3 is true.

Finally, to prove Claim 1 we estimate:

$$1 = v^T D^{-1} v \leq \|D^{-1}\|_{op}\|v\|^2 \leq \frac{1}{\kappa}|v|^2$$

Hence $|v| \geq \sqrt{\kappa}$ and the ellipsoid $\mathcal{E}_1$ contains a ball of radius $\sqrt{\kappa}$.

"$\Longleftarrow$" If the ellipsoid contains a ball of radius r, then it is non degenerate and it has n main axis e_i, with lengths α_i, $i = 1, \ldots, n$. These can be arranged such that $0 < r \leq \alpha_1 \leq \alpha_2 \leq \cdots \leq \alpha_n$. The main axis vectors are eigenvectors or generalized eigenvectors of D^{-1} with eigenvalues α_i^2, $i = 1, \ldots, n$. Then D has the same eigenvectors and generalized eigenvectors with eigenvalues $\lambda_i = \alpha_i^{-2}$, $i = 1, \ldots, n$. Then $\theta^T D\theta \geq \kappa|\theta|^2$ for

$$\kappa := \min\left\{\frac{1}{\alpha_i^2}, \imath = 1, \ldots, n\right\} = \frac{1}{\alpha_n^2}.$$

□

We show an illustration for the case of example D_1 in Figure 7.

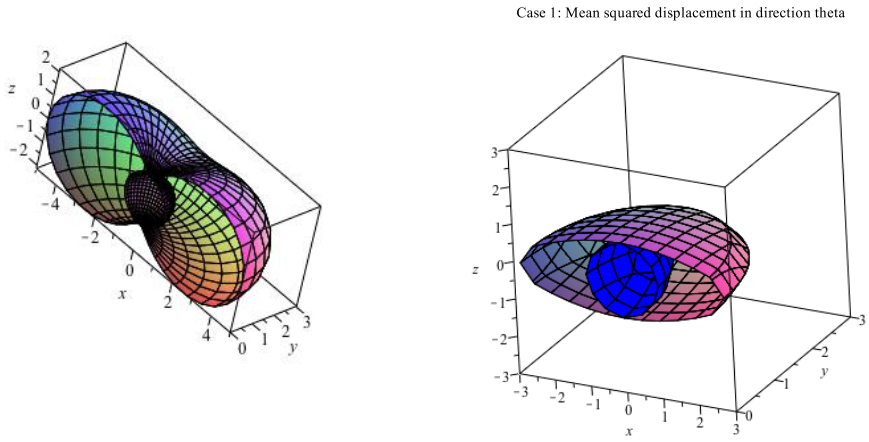

Figure 7: Left: The peanut of D_1 contains a ball. Right: The ellipsoid of case 1 contains a ball of radius 1.

5.5 Anisotropic vs. Isotropic Diffusion

Now depending on the form of the diffusion tensor D, we can obtain either *anisotropic* or *isotropic* diffusion. We call diffusion isotropic if $D = \alpha\mathbb{I}$ for some $\alpha > 0$; otherwise diffusion is called anisotropic. For isotropic diffusion the rate of spread is equivalent in all directions. The resulting distributions are spherical in nature. Anisotropic diffusion, however, occurs when the rate of diffusion varies in different directions. This can arise from many biological problems where animals have certain preferred directions of motion. The rates of spread in these directions are effectively higher, and the resulting distributions are ellipsoidal in nature, aligned with the dominant direction of spread.

In this section we will derive criteria on the turning kernel T and on the turning operator $\mathcal{L}$ which ensure that the corresponding parabolic limit is isotropic. For this we introduce the *expected velocity*

$$\bar{v}(v) := \int_V T(v, v')v'dv' \tag{44}$$

For the Pearson walk, with $V = s\mathcal{S}^{n-1}$, and $T(v, v') = \frac{1}{|V|}$we find an expected velocity of

$$\bar{v}(v) = \int_V \frac{1}{|V|}v'dv' = 0.$$

More generally, if T has the form $T(v)$, then $\bar{v}(v) = 0$ as well.

Also, if we integrate the expected velocity, then we get zero by condition (T1):

$$\int_V \bar{v}(v)dv = \int_V \int_V T(v, v')v'dv'dv = 0.$$

To decide if the diffusion limit is isotropic or anisotropic we compare three statements:

(St1) There exists an orthonormal basis $\{e_1, \ldots, e_n\} \subset \mathbb{R}^n$ such that the coordinate mappings $\phi_i : V \to \mathbb{R}, \phi_i(v) = v_i$ are eigenfunctions of $\mathcal{L}$ with common eigenvalue $\lambda \in (-2\mu, 0)$, for all $i = 1, \ldots, n$.

(St2) The expected velocity satisfies

$$\bar{v}(v) \parallel v \quad \text{and} \quad \gamma := \frac{\bar{v}(v) \cdot v}{v^2}$$

is the *adjoint persistence* with $\gamma \in (-1, 1)$.

(St3) There exists a diffusion coefficient $d > 0$ such that $D = d\mathbb{I}$ (isotropic).

Theorem 6. *Assume (T1)-(T4) and that V is symmetric w.r.t. $SO(n)$. Then we have the inclusions*

$$(St1) \quad \Leftrightarrow \quad (St2) \quad \Rightarrow (St3).$$

The constants λ, γ, d are related as

$$\gamma = \frac{\lambda + \mu}{\mu}, \quad d = -\frac{K_V}{|V|\lambda} = \frac{K_V}{|V|\mu(1-\gamma)},$$

where K_V is given by

$$\int vv^T dv = K_V \mathbb{I}.$$

Moreover, if there is a matrix M such that $\bar{v}(v) = Mv$ for all $v \in V$ then all three statements are equivalent.

Proof. (St1) $\Leftrightarrow$ (St2):

$$\begin{aligned}
\text{(St1)} &\Leftrightarrow \mathcal{L}v_i = \lambda v_i, \qquad \forall i \\
&\Leftrightarrow -\mu v_i + \mu(\bar{v}(v))_i = \lambda v_i \\
&\Leftrightarrow (\bar{v}(v))_i = \gamma v_i, \qquad \gamma = \frac{\lambda + \mu}{\mu} \\
&\Leftrightarrow \text{(St2)}
\end{aligned}$$

(St1) $\Rightarrow$ (St3): The coordinate mappings ϕ_i are eigenfunctions of $\mathcal{L}$ and $\phi_i \in \langle 1 \rangle^\perp$. Hence ϕ_i are also eigenfunctions for $\mathcal{F}$ with eigenvalue λ^{-1} for each $i = 1, \ldots, n$. Then

$$\begin{aligned} e_k D e_j &= -\frac{1}{|V|} \int_V v_k \mathcal{F} v_j dv \\ &= -\frac{1}{|V|} \frac{1}{\lambda} \int_V v_k v_j dv \\ &= -\frac{K_V}{|V|\lambda} \delta_{kj} \end{aligned}$$

(St3) $\Rightarrow$ (St1) see Hillen and Othmer [16]

□

5.5.1 Examples

Example 1, Pearson walk: As seen earlier, for the Pearson walk we have $\bar{v}(v) = 0$ and consequently also $\gamma = 0$. Still, statement (St2) is true and we find isotropic diffusion with diffusion coefficient

$$d = \frac{K_V}{|V|\mu} = \frac{s^2}{n\mu}.$$

Example 2, Symmetric T. Now we again assume $V = s\mathbb{S}^{n-1}$ but now T is symmetric of the form $T(v, v') = t(|v - v'|)$. The expected velocity

$$\bar{v}(v) = \int_V T(v, v') v' dv' = \int_V t(|v - v'|) v' dv',$$

which is not entirely trivial to compute. To do this, we consider a given $v \in V$. Since $V = s\mathbb{S}^{n-1}$ is a ball of radiaus s, the level sets

$$\Gamma_a := \{v' \in V : |v - v'| = a\}$$

are circles on $\mathbb{S}^{n-1}$ surrounding v, for $a \in (-1, 1)$. Then on Γ_a we have $t(|v - v'|) = t(a)$. Then we can split our integral

$$\begin{aligned} \int_V t(|v - v'|) v' dv' &= \int_{-1}^1 \int_{\Gamma_a} t(|v - v'|) v' dv' da \\ &= \int_{-1}^1 t(a) \int_{\Gamma_a} v' dv' \\ &= \int_{-1}^1 t(a) c_1 \, v \\ &= c_2 \, v \end{aligned}$$

where we use the fact that the symmetric integral $\int_{\Gamma_a} v'dv'$ is in direction v and c_1, c_2 are appropriate constants (note c_1 can be negative). Hence $\bar{v}(v)$ is parallel to v, and statement (St2) holds. Hence the diffusion limit is isotropic.

Example 3, nonisotropic. For this example, we will consider a constant kernel T, perturbed by a second order correction term

$$T(v, v') = \frac{1}{|V|} + v^{\mathrm{T}} \mathcal{M} v, \text{ with } \mathcal{M} \in \mathbb{R}^{n \times n} \text{ and } V = s\mathbb{S}^{n-1}.$$

Then we have

$$D = \frac{s^2}{n\mu} \left(\mathbb{I} + \frac{|V|s^2}{n} \mathcal{M} \left(\mathbb{I} - \frac{|V|s^2}{n} \mathcal{M} \right)^{-1} \right),$$

which is non- isotropic (see details in [16]).

Example 4, chemotaxis

For our last example, we will define T to be

$$T(v, v') = \frac{1}{|V|} + \epsilon Q(v, v', s) \nabla S$$

which, as we will derive in the next section, gives a chemotaxis model with

$$D = \frac{s^2}{n\mu} \text{ and } \chi(s) = \frac{1}{|V|} \int_V \int_V v Q(v, v', s) dv' ds.$$

For many more examples, see [31].

5.6 Chemotaxis

In the case of chemotaxis,tThe turning rate and the turning kernel might depend on the signal $S(x, t)$. We study these as perturbations (see [31]). Note that we cannot use v for the signal concentration, since it is used for the velocities. Hence here we use S.

$$T(v, v', S(\cdot)) = T_0(v, v') + \varepsilon^k T_1(v, v', S(\cdot)),$$

$$\mu(v, S(\cdot)) = \mu_0 + \varepsilon^\ell \mu_1(v, S(\cdot)),$$

and study the four pairwise combinations when $k, \ell = 0, 1$. We assume that T_0 satisfies (T1)-(T4), and that for T_1 we have

$$T_1 \in L^2, \qquad \int_V T_1(v, v', S(\cdot))dv = 0,$$

$$|T_1(v, v', S)| \leq T_0(v, v', S).$$

Consider then the example generated when

$$T(v, v', S(\cdot)) = T_0(v, v') + \varepsilon\alpha(S)(v \cdot \nabla S)$$

which says it is more likely to choose a new direction in the direction of ∇S. Then

$$\begin{aligned} \mathcal{L}\varphi(v) &= -\mu\varphi(v) + \mu \int_V T(v, v')\varphi(v')dv' + \varepsilon\mu\alpha(S) \int_V (v \cdot \nabla S)\varphi(v')dv' \\ &= \mathcal{L}_0\varphi(v) + \varepsilon\mu\alpha(S)(v \cdot \nabla S)\bar{\varphi}(x, t), \\ &= \mathcal{L}_0\varphi + \varepsilon\mathcal{L}_1\varphi \end{aligned}$$

where $\bar{\varphi} = \int_V \varphi dv$, and $\mathcal{L}_1\varphi = \mu\alpha(S)(v \cdot \nabla S)\bar{\varphi}(x, t)$. Because of the perturbed structure of the right hand side, we cannot directy apply the theory from above. Instead, we again compare orders of ε. The scaled transport equations is now

$$\varepsilon^2 p_t + \varepsilon v \cdot \nabla p = \mathcal{L}_0 p + \varepsilon\mathcal{L}_1 p$$

$\underline{\varepsilon^0}$**:**

$$0 = \mathcal{L}_0 p_0 \Rightarrow p_0 = p_0(x, t)$$

$\underline{\varepsilon^1}$**:**

$$v \cdot \nabla p_0 = \mathcal{L}_0 p_1 + \mathcal{L}_1 p_0$$

which is equivalent with

$$v \cdot \nabla p_0(x, t) - \mu\alpha(S)(v \cdot \nabla S)\bar{p}_0 = \mathcal{L}_0 p_1.$$

Since $\bar{p}_0 = \int_V p_0(x, t)dv = |V|p_0$ we can write this as

$$v \cdot \nabla p_0 - \mu\alpha(S)(v \cdot \nabla S)|V|p_0 = \mathcal{L}_0 p_1.$$

To solve for p_1, we need to check the solvability condition $\int_V vdv\cdot\nabla p_0 - \mu\alpha(S)\int_V vdv\cdot\nabla S p_0 = 0$, which is true due to symmetry of V. Then

$$p_1 = \mathcal{F}_0\Big(v\cdot\nabla p_0 - \mu|V|\alpha(S)(v\cdot\nabla s)p_0\Big),$$

where $\mathcal{F}_0$ is the pseudo inverse of the unperturbed part $\mathcal{L}_0$.
$\underline{\varepsilon^2}$**:**

$$p_{0t} + v\cdot\nabla p_1 = \mathcal{L}_0 p_2 + \mu\alpha(S)(v\cdot\nabla S)\bar{p}_1$$

Integrate:

$$\begin{aligned} & |V|p_{0t} + \int_V v\cdot\nabla\mathcal{F}_0\left(v\cdot\nabla p_0 - \mu|V|\alpha(S)(v\cdot\nabla S)p_0\right)dv \\ = \;& 0 + \mu\alpha(S)\underbrace{\int_V v\cdot\nabla S dv}_{=0}\bar{p}_1 \end{aligned}$$

Hence

$$|V|p_{0t} + \nabla\cdot\int_V v\mathcal{F}_0 vdv\cdot\nabla p_0 - \mu|V|\nabla\cdot\int_V v\mathcal{F}_0 vdv\cdot\alpha(S)\nabla S p_0 = 0.$$

We arrive at a (possibly anisotropic) checmotaxis equation

$$p_{0t} = \nabla\left(D\nabla p_0 - \mu|V|\alpha(S)p_0 D\nabla S\right)$$

where

$$D = -\frac{1}{|V|}\int_V v\mathcal{F}_0 vdv.$$

Notice that the diffusion tensor D appears in both terms, this means that the chemotaxis term carries the same anisotropy as the diffusion term, which it should, since the cells move in a given (possibly anisotropic) environment and both movement terms should be affected by anisotropy.

Finally, if we consider the Pearson walk with $T_0(v,v') = \frac{1}{|V|}$ and $D = \frac{s^2}{n\mu}\mathbb{I}$, then we obtain the classical (isotropic) chemotaxis model

$$p_{0t} = \nabla(d\nabla p_0 - \chi(S)p_0\nabla S$$

with $d = \frac{s^2}{n\mu}$ and $\chi(S) = \frac{|V|\alpha(S)s^2}{n}$.

5.6.1 Other cases

We considered an order ε perturbation of T in detail in the previous section. We can also consider order one perturbations, and perturbations of μ. Doing this we get into technical challenges which we skip in this manuscript. For details we refer to [31]. Here we simply list the corresponding examples

Examples:

1. In case of bacterial movement, bacteria tend to turn more often if they move down a gradient and less often if they move up a gradient. This can be expressed through a perturbed turning rate

$$\mu(S) = \mu_0(1 - \varepsilon b(S)(v \cdot \nabla S)). \tag{45}$$

   If we combine this with the Pearson walk for $T = 1/|V|$, then we obtain a chemotaxis model

$$p_{0,t} = \nabla(d\nabla p_0 - \chi(S)p_0\nabla S),$$

   with

$$\chi(S) = \frac{s^2}{n}b(S).$$

   The function $b(S)$ describes the signal sensing mechanism of the cells. Here we see how this term enters the chemotaxis model.

2. Amoeba are able to modify their turning rate as well as actively choose a favorable direction. This can be modelled by using a perturbed turing rate as above (45) as well as a perturbed turning kernel as we did above. In a special case we consider

$$T(v, v', S) = \frac{1}{|V|}(1 + \varepsilon a(S)(v \cdot S).$$

   Then we obtain a chemotaxis model with chemotactic sensitivity

$$\chi(S) = \frac{s^2}{n}(a(S) + b(S)).$$

   Hence both effects combine in a linear way.

3. If myxobacteria encounter a stream of myxobacteria moving in a given direction b, then they also turn into that direction. This can be expressed through a special kernel of

$$T(v, v') = \kappa(v \cdot b)(v' \cdot b).$$

In addition we consider the perturbed turning rate (45). The parabolic limit is of chemotaxis form

$$p_{0,t} = \nabla(D\nabla p_0 - V(p_0, S)\nabla S)$$

with nonisotropic diffusion

$$D = \frac{s^2}{\mu_0 n}\left(\mathbb{I} + \frac{|V|s^2}{n}\kappa bb^T\left(\mathbb{I} - \frac{|V|s^2}{n}\kappa bb^T\right)^{-1}\right).$$

Unfortunately, we have not been able to give a biological interpretation of this diffusion tensor.

4. It is also possible to include volume constraints into the transport equation framework. For example choosing

$$\mu(S) = \mu_0(1 - \varepsilon b(S)(v \cdot S)\beta(\int p(dv)),$$

where β is a decreasing function. Then

$$p_{0,t} = \nabla(d\nabla p_0 - p_0\beta(p_0)\chi(S)\nabla S),$$

which is the volume filling chemotaxis model as introduced by Hillen and Painter [15].

5.7 Persistence

An important biological quantity is the *persistence*. It is an indicator for the particles to keep their heading when doing a turn. A particle which never changes direction, i.e. performs a ballistic motion would have persistence 1, while a brownian particle has persistence 0. The persistence in the context of transport models is easily defined. Consider a given incoming velocity v'. Then the expected outgoing velocity is

$$\hat{v}(v') := \int_V T(v, v')v dv$$

and the average outgoing speed is

$$\hat{s} := \int_V T(v, v')\|v\| dv.$$

The *index of persistence* ψ_α is defined as

$$\psi_\alpha(v') = \frac{\hat{v} \cdot v'}{\hat{s}s'} \text{ where } s' = \|v'\|.$$

Hence the parameter γ, which we introduced in Theorem 6 is he persistence of the adjoint turning operator, or the adjoint persistence.

Homework: It is an interesting exercise to find out under which conditions is $\gamma = \psi_\alpha$. Certainly for symmetric kernel, but also for normal kernels?

5.7.1 Example

Assume that turning depends only on the relative angle

$$\theta := \arccos\left(\frac{v \cdot v'}{\|v\|\|v'\|}\right).$$

Then $T(v, v') = h(\theta(v, v')) = h(\theta - \theta'), h(-\theta) = h(\theta)$. For example, in 2-dimensions, with $s = 1$, we have $v = \binom{\cos\theta}{\sin\theta}$ and for normalization we need

$$\int_V T(v, v')dv = \int_0^{2\pi} h(\theta - \theta')d\theta = 1.$$

Which is equivalent to

$$\int_{-\theta'}^{2\pi-\theta'} h(\alpha)d\alpha = 2\int_0^{\pi} h(\alpha)d\alpha = 1.$$

The expected outgoing velocity is

$$
\begin{aligned}
\hat{v}(\theta') &= \int h(\theta-\theta')\begin{pmatrix}\cos\theta\\ \sin\theta\end{pmatrix}d\theta, \text{ and with } \alpha := \theta-\theta' \\
&= \int h(\alpha)\begin{pmatrix}\cos(\alpha+\theta')\\ \sin(\alpha+\theta')\end{pmatrix}d\alpha \\
&= \int h(\alpha)\begin{pmatrix}\cos\alpha\cos\theta'-\sin\alpha\sin\theta'\\ \sin\alpha\cos\theta'+\cos\alpha\sin\theta'\end{pmatrix}d\alpha \\
&= \begin{pmatrix}\cos\theta'\int h(\alpha)\cos\alpha d\alpha - \sin\theta'\int \underbrace{h(\alpha)\sin\alpha}_{=0}d\alpha \\ \cos\alpha'\int \underbrace{h(\alpha)\sin\alpha}_{=0}d\alpha + \sin\theta'\int h(\alpha)\cos\alpha d\alpha\end{pmatrix} \\
&= h(\alpha)\cos\alpha d\alpha\begin{pmatrix}\cos\theta'\\ \sin\theta'\end{pmatrix}.
\end{aligned}
$$

Then the persistence is given as

$$
\begin{aligned}
\psi_\alpha &= \hat{v}(\theta')\cdot v' = \int h(\alpha)\cos\alpha d\alpha(\cos\theta'\cdot\sin\theta')\begin{pmatrix}\cos\theta'\\ \sin\theta'\end{pmatrix} \\
&= \int h(\alpha)\cos\alpha d\alpha,
\end{aligned}
$$

where we can see why the persistence is sometimes called the *mean cosine*.

It is similar in 3-dimensions, where we normalize as:

$$2\pi\int_0^\pi h(\theta)\sin\theta d\theta = 1$$

and the persistence turns out to be (we skip the details):

$$\psi_\alpha = 2\pi\int_0^\pi h(\theta)\cos\theta\sin\theta d\theta$$

Again this is a mean cosine using the correct 2-dimensional surface element in 3-D: $sin\theta d\theta$.

Persistence indices are easy to measure based on the above formulas, i.e. one follows individual particle tracks and computes the mean cosine for all the turns. It has been found that slim mold *Dictyostelium discoideum* has a persistence of about $\psi_\alpha = 0.7$, whereas the persistence of *E. coli* bacteria is about $\psi_\alpha = 0.33$.

5.8 Summary and Conclusions

In this section we considered the parabolic limit of transport equations in the case of constant equilibrium distribution. The general conditions (T1)-(T4) allowed us to develop a full theory including classifications into isotropic and anisotropic diffusion and including standard chemotaxis models. However, some important examples such as $T(v, v') = q(v)$ are not included, and the question of what to do with these cases remains., and will be addressed in the following Sections.

6 Transport and Anisotropic Diffusion Models for Movement in Oriented Habitats

This section will contain the material from

- [17] T. Hillen, K. Painter, *Transport Models for Movement in Oriented Habitats and Anisotropic Diffusion.* In: Dispersal, individual movement and spatial ecology: A mathematical perspective. Eds: M.A. Lewis, P. Maini, S. Petrovskii, Heidelberg, Springer, 2012, 46 pages.
- [33] K.J. Painter, T. Hillen, *Mathematical modelling of glioma growth: the use of Diffusion Tensor Imaging (DTI) data to predict the anisotropic pathways of cancer invasion*. J. Theoretical Biol., 323, 25-39, 2013
- [14] Hillen, Thomas M^5, *Mesoscopic and Macroscopic Models for Mesenchymal Motion*, J. Math. Biol. 53(4), 585-616, 2006.

References

[1] A. Bressan. Hyperbolic Systems of Conservation Laws. Oxford University Press, 2000.

[2] C. Cercignani, R. Illner, and M. Pulvirenti. The Mathematical Theory of Diluted Gases. Springer, New York, 1994.

[3] J.C. Dallon and H.G. Othmer. A discrete cell model with adaptive signalling for aggregation of dictyostelium discoideum. Phil. Trans. R. Soc. Lond. B, 352:391–417, 1997.

[4] R. Dautray and J.-L. Lions. Mathematical Analysis and Numerical Methods for Science and Technology. Springer, Heidelberg, 2000.

[5] G. A. Dunn and J. P. Heath. A new hypothesis of contact guidance in tissue cells. Exp. Cell Res., 101(1):1–14, 1976.

[6] R. Eftimie. Hyperbolic and kinetic models for self-organized biological aggregations and movement: a brief review. J. Math. Biol., 65(1):35–75, 2012.

[7] R. Erban and H. Othmer. From signal transduction to spatial pattern formation in *e. coli*: a paradigm for multiscale modeling in biology. Multiscale Modeling and Simulation, 3(2):362–394, 2005.

[8] R. Fürth. Die brownsche bewegung bei berücksichtigung einer persistenz der bewegungsrichtung. Zeitschrift für Physik, 2:244–256, 1920.

[9] A. Giese, R. Bjerkvig, M.E. Berens, and M. Westphal. Cost of migration: invasion of malignant gliomas and implications for treatment. Journal of Clinical Oncology, 21(8):1624–1636, 2003.

[10] A. Giese, L. Kluwe, B. Laube, H. Meissner, M. E. Berens, and M. Westphal. Migration of human glioma cells on myelin. Neurosurgery, 38(4):755–764, 1996.

[11] S. Goldstein. On diffusion by discontinuous movements and the telegraph equation. Quart. J. Mech. Appl. Math., 4:129–156, 1951.

[12] P.R. Halmos and V.S. Sunder. Bounded Integral Operators on L2 Spaces. Springer, Heidelberg, 1978.

[13] T. Hillen. On the L^2-closure of transport equations: The general case. Discrete and Cont. Dyn. Syst. Series B, 5(2):299–318, 2005.

[14] T. Hillen. M^5 mesoscopic and macroscopic models for mesenchymal motion. Journal of Mathematical Biology, 53:585–616, 2006.

[15] T. Hillen. Existence theory for correlated random walks on bounded domains. CAMQ, (Canad. Appl. Math. Quart.), 18(1):1–40, 2010.

[16] T. Hillen and H.G. Othmer. The diffusion limit of transport equations derived from velocity jump processes. SIAM J. Appl. Math., 61(3):751–775, 2000.

[17] T. Hillen and K. Painter. Transport and anisotropic diffusion models for movement in oriented habitats. In M. Lewis, P. Maini, and S. Petrovskii, editors, Dispersal, individual movement and spatial ecology: A mathematical perspective, page 46, Heidelberg, 2012. Springer.

[18] T. Hillen and K.J. Painter. A user's guide to PDE models for chemotaxis. J. Math. Biol., 58:183–217, 2009.

[19] T. Hillen, C. Rohde, and F. Lutscher. Existence of weak solutions for a hyperbolic model for chemosensitive movement. J. Math. Anal. Appl., 260:173–199, 2001.

[20] T. Hillen and A. Stevens. Hyperbolic models for chemotaxis in 1-d. Nonlinear Analysis: Real World Applications, 1(1):409–433, 2001.

[21] D. Horstmann. From 1970 until present: The Keller-Segel model in chemotaxis and its consequences I. Jahresberichte der DMV, 105(3):103–165, 2003.

[22] D.D. Joseph and L. Preziosi. Heat waves. Reviews of Modern Physics, 61:41–73, 1988.

[23] M. Kac. A stochastic model related to the telegrapher's equation. Rocky Mountain J. Math., 4:497–509, 1956.

[24] E.F. Keller and L.A. Segel. Initiation of slime mold aggregation viewed as an instability. J. theo. Biology, 26:399–415, 1970.

[25] M.A. Krasnoselskii. Positive Solutions of Operator Equations. P. Noordhoff, Groningen, The Netherlands, 1964. English translation of Russian original.

[26] H.W. McKenzie. Linear features impact predator-prey encounters: analysis and first passage time, 2006. MSc thesis, University of Alberta.

[27] H.W. McKenzie, E.H. Merrill, R.J. Spiteri, and M.A. Lewis. How linear features alter predator movement and the functional response. 2011. submitted.

[28] V. Nanjundiah. Chemotaxis, signal relaying and aggregation morphology. J. Theoretical Biology, 42:63–105, 1973.

[29] A. Okubo and S.A. Levin. Diffusion and Ecological Problems: Modern Perspectives. Springer, 2002.

[30] H.G. Othmer, S.R. Dunbar, and W. Alt. Models of dispersal in biological systems. J. Math. Biol., 26:263–298, 1988.

[31] H.G. Othmer and T. Hillen. The diffusion limit of transport equations II: Chemotaxis equations. SIAM J. Appl. Math., 62(4):1122–1250, 2002.

[32] H.G. Othmer and C. Xue. Multiscale models of taxis-driven patterning in bacterial populations. SIAM Appl. Math., 70(1):133–167, 2009.

[33] K.J. Painter and T. Hillen. Mathematical modelling of glioma growth: the use of diffusion tensor imaging DTI data to predict the anisotropic pathways of cancer invasion. J. Theor. Biol., 323:25–39, 2013.

[34] A. Pazy. Semigroups of Linear Operators and Applications to Partial Differential Equations. Springer, New York, 1983.

[35] D.W. Stroock. Some stochastic processes which arise from a model of the motion of a bacterium. Probab. Theory Rel. Fields, 28:305–315, 1974.

[36] G.I. Taylor. Diffusion by discontinuous movements. Proc. London Math. Soc., pages 25–70, 1920.

[37] M.E. Taylor. Partial Differential Equations III. Springer, New York, 1996.

[38] M.L. Ware, M.S. Berger, and D.K. Binder. Molecular biology of glioma tumorgenesis. Histology and Histopathology, 18:207–216, 2003.

[39] E. Zauderer. Partial Differential Equations. Wiley, Hoboken, 3 edition, 2006.